IDENTIFICATION AND ATMOSPHERIC REACTIONS OF POLAR PRODUCTS OF SELECTED AROMATIC HYDROCARBONS

Final Report to California Air Resources Board
Contract No. 03-319
for the period March 1, 2004 to July 31, 2006

Roger Atkinson and Janet Arey, Co-Principal Investigators

Air Pollution Research Center
University of California
Riverside, CA 92521

July 2006

DISCLAIMER

The statements and conclusions in this Report are those of the contractor and not necessarily those of the California Air Resources Board. The mention of commercial products, their sources, or their use in connection with material reported herein is not to be construed as actual or implied endorsement of such products.

ACKNOWLEDGEMENTS

We thank the following for their contributions to the research described in this report:

Ms. Sara M. Aschmann
Dr. Ernesto C. Tuazon
Ms. Noriko Nishino
Mr. William D. Long

and thank Drs. Eileen McCauley and William Vance (CARB) for their assistance and advice during this contract.

This Report was submitted in fulfillment of Contract No. 03-319, "Identification and Atmospheric Reactions of Polar Products of Selected Aromatic Hydrocarbons" under the sponsorship of the California Air Resources Board. Work was completed as of July 15, 2006.

TABLE OF CONTENTS

LIST OF FIGURES

Page

LIST OF TABLES

ABSTRACT

During this experimental program, we have used the facilities and expertise available at the Air Pollution Research Center, University of California, Riverside, to investigate the atmospheric chemistry of selected aromatic hydrocarbons found in California's atmosphere. Experiments were carried out in large volume (5800 to ~7500 liter) chambers with analysis of reactants and products by gas chromatography (with flame ionization and mass spectrometric detection) and *in s*itu Fourier transform infrared spectroscopy. The gas chromatographic analyses included the use of Solid Phase MicroExtraction (SPME) fibers coated with derivatizing agent for on-fiber derivatization of carbonyl-containing compounds, with subsequent gas chromatographic (GC) analyses of the carbonyl-containing compounds as their oximes. This technique was especially useful for the identification and quantification of 1,2-dicarbonyls and unsaturated 1,4-dicarbonyls, some of which are not commercially available and most of which and do not elute from gas chromatographic columns without prior derivatization.

We showed that the OH radical-initiated reaction of 3-methyl-2-butenal in the presence of NO is a good *in situ* source of gaseous glyoxal which can be routinely used for calibration of the SPME fiber sampling for the quantitative analysis of glyoxal from other reaction systems (and this reaction is now being used by other research groups for that purpose). We have observed the formation of a series of 1,2-dicarbonyls and unsaturated 1,4-dicarbonyls from the OH radical-initiated reactions of toluene, *o*-, *m*- and *p*-xylene and 1,2,3-, 1,2,4- and 1,3,5,-trimethylbenzene. The observation of these products as their di-oximes shows that they are indeed present in their dicarbonyl form and not as isomeric furanones.

The second major task involved investigation of the dependence of the formation yields of selected products of the OH radical-initiated reactions of toluene, naphthalene and biphenyl as a function of the NO_x concentration; specifically, formation of glyoxal from naphthalene and formation of 3-nitrotoluene, 1- and 2-nitronpahthalene and 3-nitrobiphenyl from toluene, naphthalene and biphenyl, respectively. We measured the formation yields of glyoxal from the reaction of OH radicals with naphthalene as a function of the initial NO_x concentration, using the photolysis of methyl nitrite in air to generate OH radicals in the presence of NO_x and the dark reaction of O_3 with 2-methyl-2-butene to generate OH radicals in the absence of NO_x. We showed that glyoxal is a first-generation product, with no obvious evidence for a change in the glyoxal formation yield with initial NO_x concentration over the range <0.1-5 ppmv.

A more direct investigation of the effect of NO_x on product formation was initiated by studying the formation of 3-nitrotoluene, 1- and 2-nitronaphthalene and 3-nitrobiphenyl from the OH radical-initiated reactions of toluene, naphthalene and biphenyl, respectively. Analytical methods and procedures were developed to analyze for these nitro-aromatics at the low concentrations expected to be formed from these reactions, and the procedures developed were used to study formation of 3-nitrotoluene from the toluene reaction. Our results are in excellent agreement with laboratory kinetic data concerning the functional form of the dependence of the 3-nitrotoluene formation yield on NO_x concentration over the range 0.02-10 ppmv, showing that we have a quantitative understanding of the reactions involved in 3-nitrotoluene formation.

The data obtained in this Contract will prove important for including into chemical mechanisms for modeling photochemical air pollution and the formation of nitroaromatics in the atmosphere. Additional work is needed to complete investigation of the formation of nitro-PAHs (and specifically 1- and 2-nitronaphthalene and 3-nitrobiphenyl) under atmospheric conditions and to compare these laboratory predictions with ambient atmospheric measurements of nitro-aromatics and their parent aromatic hydrocarbons.

EXECUTIVE SUMMARY

During this experimental program, we used the facilities and expertise available at the Air Pollution Research Center, University of California, Riverside, to investigate the atmospheric chemistry of selected volatile organic compounds found in California's atmosphere. Experiments were carried out in large volume (5800 to ~7500 liter) chambers with analysis of reactants and products by gas chromatography (with flame ionization and mass spectrometric detection) and *in s*itu Fourier transform infrared spectroscopy. The gas chromatographic analyses included the use of Solid Phase MicroExtraction (SPME) fibers coated with derivatizing agent for on-fiber derivatization of carbonyl-containing compounds, with subsequent gas chromatographic analyses of the carbonyl-containing compounds as their oximes.

We used precoated SPME fibers for analysis of carbonyl-containing products from the OH radical-initiated reactions of toluene, *o*-, *m*- and *p*-xylene and 1,2,3,-, 1,2,4- and 1,3,5-trimethylbenzene at NO_2 concentrations such that the OH-aromatic adducts were reacting dominantly with O_2 (as in ambient air). The 1,2-dicarbonyls and unsaturated 1,4-dicarbonyls listed in Table ES-1 were observed as their mono-oximes, di-oximes, or mono- and di-oximes. In addition, aldehydes formed after H-atom abstraction from the substituent methyl group(s) were observed as their mono-oximes. Our data show that sets of 1,2-dicarbonyl + unsaturated 1,4-dicarbonyl products are formed, although we do not observe all possible such sets of products, nor was there any evidence for the presence of di-unsaturated 1,6-dicarbonyls, unsaturated epoxy-1,6-dicarbonyls or of epoxycyclohexenones.

Table ES-1. Ring-opened dicarbonyls observed and their assignments

	toluene	xylene			trimethylbenzene		
ring-opened product		*o*-	*m*-	*p*-	1,2,3-	1,2,4-	1,3,5-
$(CHO)_2$	•	•	•	•	•	•	
$CH_3C(O)CHO$	•	•	•	•	•	•	•
$CH_3C(O)C(O)CH_3$		•			•	•	
HC(O)CH=CHCHO	•	•					
$CH_3C(O)CH{=}CHCHO$	•	•	•		•		
$CH_3C(O)C(CH_3){=}CHCHO$		•			•	•	
$CH_3C(O)CH{=}CHC(O)CH_3$				•		•	
$CH_3C(O)CH{=}C(CH_3)CHO$							•

The second major task involved investigation of the dependence of the formation yields of selected products of the OH radical-initiated reactions of toluene, naphthalene and biphenyl as a function of the NO_x concentration; specifically, formation of glyoxal from naphthalene and formation of 3-nitrotoluene, 1- and 2-nitronpahthalene and 3-nitrobiphenyl from toluene, naphthalene and biphenyl, respectively. Our initial work on this task was to find an *in situ* source of glyoxal for routine, quantitative calibration of our SPME fiber sampling. We investigated the kinetics and products of the reaction of OH radicals with 3-methyl-2-butenal in the presence of NO, using *in situ* FT-IR analysis and SPME/GC-FID analysis. The results are shown in Table ES-2.

Table ES-2. Products observed, and their formation yields, from the OH radical-initiated reaction of 3-methyl-2-butenal in the presence of NO

product	molar formation yield (%)[a]	analysis method
acetone	74 ± 6	FT-IR
glyoxal	40 ± 3	FT-IR
2-hydroxy-2-methylpropanal	4.6 ± 0.7	SPME/GC-FID
CO_2	39-30	FT-IR
$RC(O)OONO_2$	5-8	FT-IR
$RONO_2$	8.5 ± 2.3	FT-IR

[a]Indicated errors are two least-squares standard deviations combined with estimated uncertainties in the FT-IR calibrations or SPME/GC-FID response factors.

This reaction is rapid, with a measured room temperature rate constant of 6.2 x 10^{-11} cm^3 $molecule^{-1}$ s^{-1}, and it has a 40 ± 3% yield of glyoxal. Accordingly, we (and other research groups) are now using this reaction as a convenient source of known concentrations of gaseous glyoxal for calibration purposes.

We measured the formation yields of glyoxal from the reaction of OH radicals with naphthalene as a function of the initial NO_x concentration, using the photolysis of methyl nitrite in air to generate OH radicals in the presence of NO_x and the dark reaction of O_3 with 2-methyl-2-butene to generate OH radicals in the absence of NO_x. We showed that glyoxal is a first-generation product, and that there is no obvious evidence for a change in the glyoxal formation yield with NO_x concentration (Figure ES-1), with an average glyoxal yield of 6 ± 2% independent of initial NO_x over the range <0.1-5 ppmv.

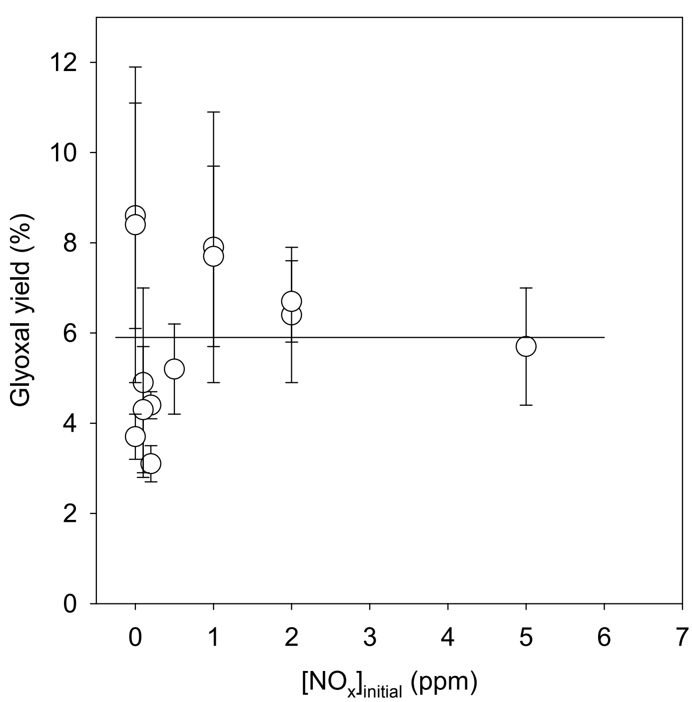

Figure ES-1. Plot of glyoxal formation yield from the reaction of OH radicals with naphthalene as a function of the initial NO_x concentration.

A more direct investigation of the effect of NO_x on product formation was initiated by studying the formation of 3-nitrotoluene, 1- and 2-nitronaphthalene and 3-nitrobiphenyl from the OH radical-initiated reactions of toluene, naphthalene and biphenyl, respectively. Analytical methods and procedures were developed to analyze for these nitro-aromatics at the low concentrations expected to be formed from these reactions, and the procedures employed to study the formation of 3-nitrotoluene from the toluene reaction. Our results (in arbitrary units) are shown in Figure ES-2 together with a fit based on the literature rate constants for the reactions of the intermediate OH-toluene adduct(s) with O_2 and NO_2. The excellent agreement between laboratory kinetic and mechanistic data and product yield data concerning the functional form of the 3-nitrotoluene formation yield dependence on NO_x concentration over the range 0.02-10 ppmv shows that we have a quantitative understanding of the reactions leading to atmospheric formation of 3-nitrotoluene from toluene.

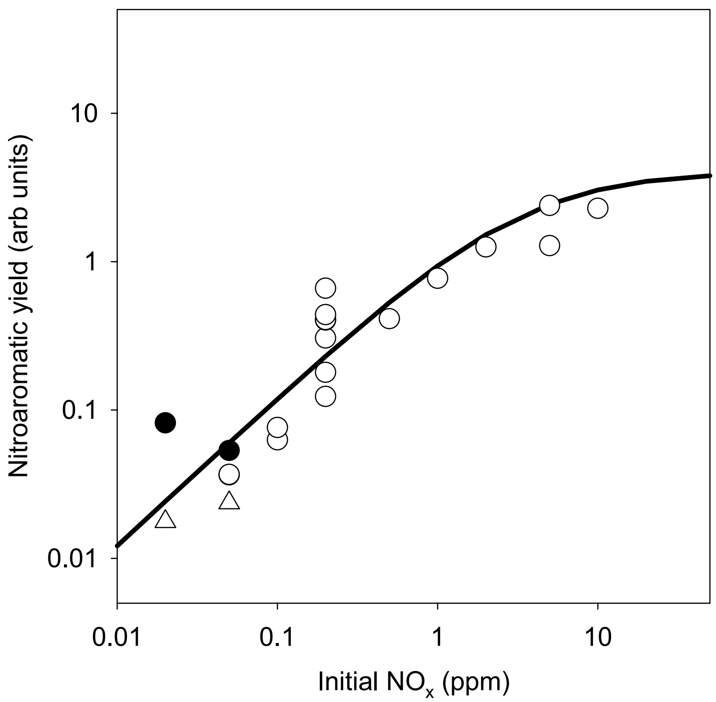

Figure ES-2. Plot of the 3-nitrotoluene formation yield (arbitrary units) against the initial NO_x concentration. The line is based on rate constants for the reactions of the OH-toluene adducts with O_2 and NO_2.

The data obtained in this Contract will prove important for including into chemical mechanisms for modeling photochemical air pollution and the formation of nitroaromatics in the atmosphere. Additional work is needed to complete investigation of the formation of nitro-PAHs (and specifically 1- and 2-nitronaphthalene and 3-nitrobiphenyl) under atmospheric conditions and to compare these laboratory predictions with ambient atmospheric measurements of nitro-aromatics and their parent aromatic hydrocarbons.

I. INTRODUCTION AND BACKGROUND

Monocyclic aromatic hydrocarbons and polycyclic aromatic hydrocarbons (PAHs) are present in gasoline and diesel fuels (Williams et al., 1989; Hoekman, 1992; Marr et al., 1999; Zielinska et al., 2004), and are emitted into the atmosphere from volatilization during fuel usage and from vehicle exhaust (Williams et al., 1989; Hoekman, 1992; Fraser et al., 1998; Marr et al., 1999; Zielinska et al., 2004). While aromatic hydrocarbons and PAHs are formed during the combustion process, the monocyclic aromatic hydrocarbons and alkylated-PAH species present in vehicle emissions may be largely from unburned fuel (Williams et al., 1989; Tancell et al., 1995; Fraser et al., 1998). In the atmosphere, the most abundant aromatic hydrocarbons are benzene and the C_1-C_3 alkylbenzenes (toluene, xylenes, ethylbenzene, trimethylbenzenes and ethyltoluenes) among the monocyclic aromatic hydrocarbons, and naphthalene, 1- and 2-methylnaphthalene and ethyl- and dimethylnaphthalenes among the PAHs (Calvert et al., 2002; Reisen et al., 2003a; Reisen and Arey, 2005).

These $\leq C_3$-alkylbenzenes and $\leq C_2$-alkylnaphthalenes are sufficiently volatile that they are present essentially entirely in the gas phase in the lower troposphere (Bidleman, 1988; Wania and Mackay, 1996; Arey and Atkinson, 2003). In the atmosphere, benzene and the alkylbenzenes and naphthalene and the alkylnaphthalenes react with OH radicals during daylight hours and with NO_3 radicals during evening and nighttime hours (Arey, 1998; Calvert et al., 2002; Arey and Atkinson, 2003; Atkinson and Arey, 2003). Table 1 gives the room temperature rate constants for the reactions of OH radicals and NO_3 radicals with these monocyclic aromatic hydrocarbons and PAHs. Table 2 gives the calculated tropospheric lifetimes due to reaction with OH radicals and NO_3 radicals using a 12-hr average daytime OH radical concentration of 2.0×10^6 cm^{-3} (Prinn et al., 2001; Krol and Lelieveld, 2003) and a 12-hr average nighttime NO_3 radical concentration of 5×10^8 cm^{-3} (Atkinson, 1991). Note that the calculated lifetimes are inversely proportional to the assumed OH radical concentration or NO_3 radical concentration or, for the PAHs, to the product of the NO_3 and NO_2 concentrations (see below). It should be recognized that the major sources of OH radicals in the troposphere are photolytic and hence the OH radical concentrations depend on a number of factors including time of day, season and latitude, and cloud cover. NO_3 radical concentrations are highly spatially and temporally variable with the measured maximum nighttime concentrations varying from $<5 \times 10^7$ cm^{-3} to 1×10^{10} cm^{-3} (Atkinson et al., 1986). The calculated lifetimes in Table 2 indicate that the OH radical reactions are the dominant atmospheric loss process for these compounds. Aromatic hydrocarbons typically comprise ~20% of the non-methane VOCs in urban areas (Calvert et al., 2002) and are calculated to account for ~40% of the ozone-forming potential, based on their maximum incremental reactivity (MIR) factors (Calvert et al., 2002). Moreover, aromatic hydrocarbons are believed to be the dominant class of VOCs with respect to secondary organic aerosol formation in urban areas (Odum et al., 1997).

Table 1. Room temperature rate constants k (cm^3 $molecule^{-1}$ s^{-1}) for the reaction of OH radicals and NO_3 radicals with benzene, $\leq C_3$ alkylbenzenes and naphthalene and $\leq C_2$ alkylnaphthalenes.

Monocyclic aromatic	reaction with OH 10^{12} x k^a	reaction with NO_3 10^{16} x k^a
benzene	1.22	<0.3
toluene	5.63	0.70
toluene-d_3 [$C_6H_5CD_3$]	5.63[b]	0.38[d]
toluene-d_8 [$C_6D_5CD_3$]	6.31[b]	0.34[d]
ethylbenzene	7.0	<6
o-xylene	13.6	4.1
m-xylene	23.1	2.6
p-xylene	14.3	5.0
n-propylbenzene	5.8	
isopropylbenzene	6.3	
o-ethyltoluene	11.9	
m-ethyltoluene	18.6	
p-ethyltoluene	11.8	
1,2,3-trimethylbenzene	32.7	19
1,2,4-trimethylbenzene	32.5	18
1,3,5-trimethylbenzene	56.7	8.8
PAH	reaction with OH 10^{12} x k^a	reaction with NO_3 10^{28} x k[NO_2]
naphthalene	23.9[c]	3.65[e]
1-methylnaphthalene	40.9[c]	7.15[e]
2-methylnaphthalene	48.6[c]	10.2[e]
1-ethylnaphthalene	36.4[c]	9.82[e]
2-ethylnaphthalene	40.2[c]	7.99[e]
1,2-dimethylnaphthalene	59.6[c]	64.0[e]
1,3-dimethylnaphthalene	74.9[c]	21.3[e]
1,4-dimethylnaphthalene	57.9[c]	13.0[e]
1,5-dimethylnaphthalene	60.1[c]	14.1[e]
1,6-dimethylnaphthalene	63.4[c]	16.5[e]
1,7-dimethylnaphthalene	67.9[c]	13.5[e]
1,8-dimethylnaphthalene	62.7[c]	212[e]
2,3-dimethylnaphthalene	61.5[c]	15.2[e]
2,6-dimethylnaphthalene	66.5[c]	21.2[e]
2,7-dimethylnaphthalene	68.7[c]	21.0[e]

[a]From Atkinson and Arey (2003), unless noted otherwise.
[b]From Atkinson (1989).
[c]From Phousongphouang and Arey (2002).
[d]From Atkinson (1991).
[e]From Phousongphouang and Arey (2003a).

Table 2. Ranges of tropospheric lifetimes for benzene, $\leq C_3$ alkylbenzenes and naphthalene and $\leq C_2$ alkylnaphthalenes calculated for reactions with OH radicals and NO_3 radicals.

aromatic	lifetime due to reaction with	
	OH radical[a]	NO_3 radical[b]
benzene	9.5 day	>4 yr
toluene	2.1 day	1.8 yr
xylenes	6.0-10 hr	93-178 day
trimethylbenzenes	2.4-4.3 hr	24-53 day
naphthalene	5.8 hr	52 day[c]
methylnaphthalenes	2.9-3.4 hr	18-26 day[c]
dimethylnaphthalenes	1.9-2.4 hr	0.9-14 day[c]

[a]Calculated using a 12-hr daytime average OH radical concentration of 2.0×10^6 molecule cm^{-3}.
[b]Calculated using a 12-hr nighttime average NO_3 radical concentration of 5×10^8 molecule cm^{-3}.
[c]Reaction rate also depends on the NO_2 concentration (see text). Lifetimes have been calculated using an average NO_2 concentration of 2.46×10^{12} molecule cm^{-3} (100 ppbv mixing ratio), which would represent a heavily polluted airmass.

While the rate constants for the gas-phase reactions of OH radicals and NO_3 radicals with many of the simple monocyclic aromatic hydrocarbons (benzene and the C_1-C_3 alkylbenzenes) and with naphthalene and the C_1-C_2 alkylnaphthalenes have been measured (Table 1), the detailed mechanisms of these OH radical- and NO_3 radical-initiated reactions in the atmosphere are less well understood, especially for the PAHs, and the elucidation of selected aspects of their chemical mechanisms was the focus of this contract. For convenience, in the sections below we refer to benzene and the C_1-C_3 alkylbenzenes (toluene, xylenes, ethylbenzene, trimethylbenzenes, ethyltoluenes and propylbenzenes) as monocyclic aromatic hydrocarbons, and to naphthalene and the C_1-C_2 alkyl naphthalenes (methyl-, ethyl- and dimethyl-naphthalenes) as PAHs.

OH Radical Reactions

Kinetic and product studies show that for both monocyclic aromatic hydrocarbons and PAHs, the OH radical reactions proceed mainly by OH radical addition to the aromatic ring(s) at room temperature and below (Atkinson, 1989). At elevated temperatures, the reactions proceed by H-atom abstraction from the C-H bonds, mainly from the C-H bonds of the substituent alkyl groups (Atkinson, 1989). For example, for toluene the OH radical reaction proceeds as shown in Scheme 1, with the hydroxymethylcyclohexadienyl radical (hereafter termed an "OH-aromatic adduct" or, for the corresponding reaction with PAHs, an "OH-PAH adduct") back-decomposing to reactants at elevated temperature. The "M" shown in Scheme 1 indicates the requirement for a "third-body" to thermalize the adduct and while the room temperature rate constants for benzene and toluene are in the fall-off regime (where the adducts are not completely thermalized) at pressures ≤100 Torr (Atkinson, 1989), at atmospheric pressure of air the rate constants for benzene and toluene are within ~5% of the high-pressure limiting values and those for the ≥C_2 alkylbenzenes should be at the high-pressure limit at atmospheric pressure (Atkinson, 1989). In the discussion below, kinetic and product data applicable to atmospheric pressure of air are used.

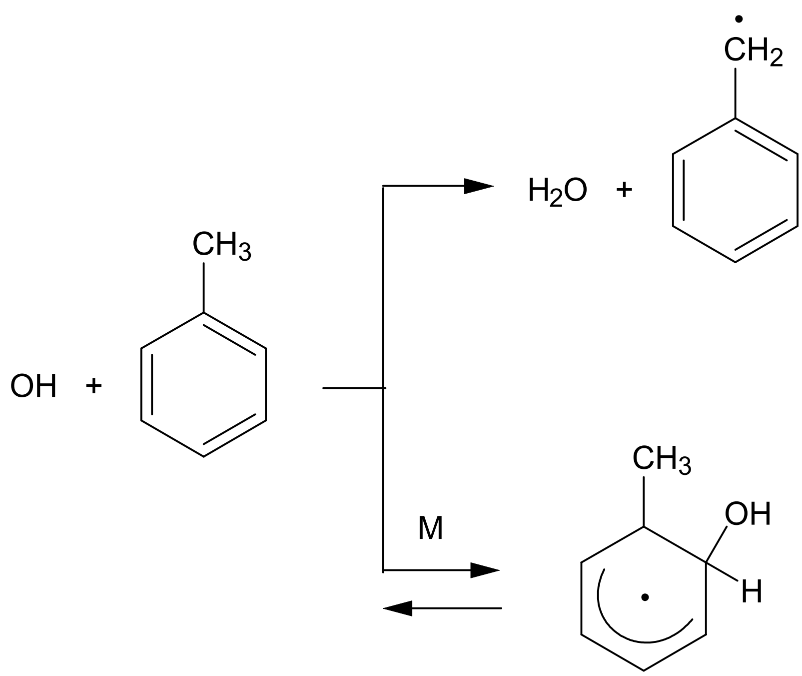

Scheme 1

Kinetic and product data show that the OH radical addition pathway, to form an OH-aromatic adduct, dominates, accounting for >90% of the overall reaction at room temperature and atmospheric pressure of air for benzene, toluene, the xylenes and the trimethylbenzenes (Atkinson, 1989). The minor H-atom abstraction pathway leads to the formation (Scheme 1) of benzyl or alkylbenzyl radicals, which react further by a series of reactions analogous to those for alkyl radicals (Atkinson and Arey, 2003) to form benzaldehyde or alkylbenzaldehydes and benzyl nitrate or alkylbenzyl nitrates (Atkinson, 1994). For the methylnaphthalenes, the naphthaldehyde yields suggest that <5% of the room temperature reaction is due to H-atom abstraction (Atkinson et al., 1997). The products formed from the OH-aromatic adducts are discussed below.

Reactions of the OH-Aromatic and OH-PAH Adducts

OH-Aromatic Adducts. The hydroxy-alkylcyclohexadienyl radicals (or OH-aromatic adducts) are now known to react with O_2 and NO_2 (Knispel et al., 1990; Koch et al., 1994; Bohn and Zetzsch, 1999; Bohn, 2001). For the OH-benzene, OH-toluene and OH-*p*-xylene adducts, the room temperature rate constants for reaction with O_2 are in the range (2-8) x 10^{-16} cm^3 $molecule^{-1}$ s^{-1} (Knispel *et al*., 1990; Koch *et al*., 1994; Bohn and Zetzsch, 1999; Bohn, 2001), with these rate constants being those for an irreversible reaction with the OH-aromatic adduct and/or the OH-aromatic-O_2 species [see Bohn and Zetzsch (1999) and Bohn (2001) and Scheme 2 for the reactions of the OH-toluene adduct with O_2 below]. Bohn and Zetzsch (1999) and Bohn (2001) have shown that the OH-benzene and OH-toluene adducts reversibly add O_2 to form OH-benzene-O_2 and OH-toluene-O_2 peroxy radicals, with equilibrium concentrations of the OH-aromatic adducts and the OH-aromatic-O_2 peroxy radicals being comparable at 298 K and atmospheric pressure of air.

As noted above, an irreversible reaction of the OH-aromatic adducts with O_2 with an "effective" rate constant of (2-8) x 10^{-16} cm^3 $molecule^{-1}$ s^{-1} is observed. This irreversible removal of the OH-aromatic adduct in the presence of O_2 can be due to an irreversible reaction of the OH-aromatic adduct with O_2, with rate constants for the OH-benzene and OH-toluene adducts of 2 x 10^{-16} cm^3 $molecule^{-1}$ s^{-1} and 6.0 x 10^{-16} cm^3 $molecule^{-1}$, respectively, or to a first-order removal reaction of the OH-benzene-O_2 and OH-toluene-O_2 species with rates of ~760 s^{-1} and ~1850 s^{-1}, respectively, or any combination of these two extremes (Bohn and Zetzsch, 1999; Bohn, 2001).

For the OH-benzene, OH-toluene and OH-*p*-xylene adducts, the room temperature rate constants for reaction with NO_2 are ~3 x 10^{-11} cm^3 $molecule^{-1}$ s^{-1} (Knispel *et al*., 1990; Koch *et al*., 1994). The magnitude of the rate constants for the reactions of OH-aromatic adducts with O_2 (the irreversible process) and with NO_2 indicate that the OH-aromatic adducts will react almost exclusively with O_2 in the troposphere, but that reaction with NO_2 can become important in laboratory studies conducted at high NO_x concentrations [the O_2 and NO_2 reactions are of equal importance at atmospheric pressure of air at an NO_2 concentration of (3-13) x 10^{13} molecule cm^{-3} (a mixing ratio of ~1-5 parts-per-million)].

OH-PAH Adducts. In contrast to the situation for the monocyclic aromatic hydrocarbons, there are no published data concerning the reaction of the OH-PAH adducts with O_2 and with NO_2. Gas-phase OH and NO_3 radical-initiated reactions have been used to explain the ubiquitous presence of 2-nitrofluoranthene in ambient air (Arey, 1998; Arey and Atkinson, 2003; Atkinson and Arey, 2003). Despite the fact that 2-nitrofluoranthene has not been observed in significant quantities in emissions such as diesel exhaust, which is known to be a significant source of the isomeric nitro-PAH 1-nitropyrene, 2-nitrofluoranthene is often the most abundant particle-associated nitro-PAH in ambient samples (see Reisen and Arey (2005) for a detailed discussion and references) and it has been identified in laboratory studies from both OH radical and NO_3 radical-initiated reactions of gas-phase fluoranthene (Arey, 1998; Arey and Atkinson, 2003).

The semi-volatile nitro-PAHs are more abundant than the particle-associated nitro-PAHs (Reisen and Arey, 2005) and 1- and 2-nitronaphthalene, methylnitronaphthalenes and ethyl-/dimethyl-nitronaphthalenes are observed in ambient air with relative concentrations and isomer profiles reasonably consistent with their formation from OH (and NO_3) radical-initiated reactions (Arey et al., 1987, 1989; Zielinska et al., 1989; Gupta et al., 1996; Reisen et al., 2003a; Reisen and Arey, 2005). For example, Figure 1 shows the profile of methylnitronaphthalenes as analyzed by gas chromatography-mass spectrometry (GC-MS) with negative ion chemical ionization (NCI) at 187 da, from reaction of 1- and 2-methylnaphthalene (in a 1:2 ratio mimicking their ambient concentrations) with OH radicals in an environmental chamber (top trace) and from an ambient air sample collected during morning hours in Mexico City during the MCMA 2003 (de Foy et al., 2005; Marr et al., 2006) sampling campaign (2nd trace). The Mexico City methylnitronaphthalene (*x*M*y*NN) profile strongly resembles the chamber OH radical-initiated reaction, and 1M5NN is the most prominent peak on both traces. The smaller 2M1NN peak in the Mexico City ambient sample is explained by photolysis of 2M1NN in the atmosphere (photolysis was unimportant in our short duration chamber reaction). The methylnitronaphthalenes photolyze rapidly, with lifetimes ranging from ~6 and ~10 min for 1M8NN and 2M1NN, respectively, to ~133 min for 2M6NN based on an average 12-hr daytime light intensity (Phousongphouang and Arey, 2003b). A semi-quantitative analysis of our previous ambient air data for nitro-PAH formed from volatile PAH is given in section (B) below.

II. OVERALL OBJECTIVES

There were two major questions which we attempted to answer during this contract, as follows:

- What are the reaction products formed from the reactions of the OH-monocyclic aromatic adducts with O_2 (i.e., under atmospheric conditions)?

- What is the relative importance of the reactions of OH-PAH adducts with O_2 and NO_2, and do the OH-PAH adducts react to a significant extent with NO_2 even at the ambient NO_2 concentrations characteristic of urban airmasses?

For convenience, for each of these general objectives below, (A) Carbonyl Products of the OH Radical-Initiated Reactions of a Series of Monocyclic Aromatic Hydrocarbons, and (B) Effect of NO_x Concentrations on the Yields of Selected Products formed from the OH Radical-Initiated reactions of Naphthalene, we give an Introduction, Specific Objectives and Research and Discussion section.

A. Carbonyl Products of the OH Radical-Initiated Reactions of a Series of Monocyclic Aromatic Hydrocarbons

1. Introduction

The products observed from the OH radical-initiated reactions of benzene and methyl-benzenes are (Atkinson and Arey, 2003 and references therein): aromatic aldehydes and benzyl nitrates formed after initial H-atom abstraction; phenolic compounds; one or more sets of 1,2-dicarbonyl + unsaturated 1,4-dicarbonyl; di-unsaturated 1,6-dicarbonyls; unsaturated epoxy-1,6-dicarbonyls, and epoxycyclohexenones. The evidence for the formation of di-unsaturated 1,6-dicarbonyls; unsaturated epoxy-1,6-dicarbonyls, and epoxycyclohexenones under atmospheric conditions is based on qualitative analyses by atmospheric pressure ionization mass spectrometry (Kwok et al., 1997) and derivatization/combined gas chromatography-mass spectrometry (Yu et

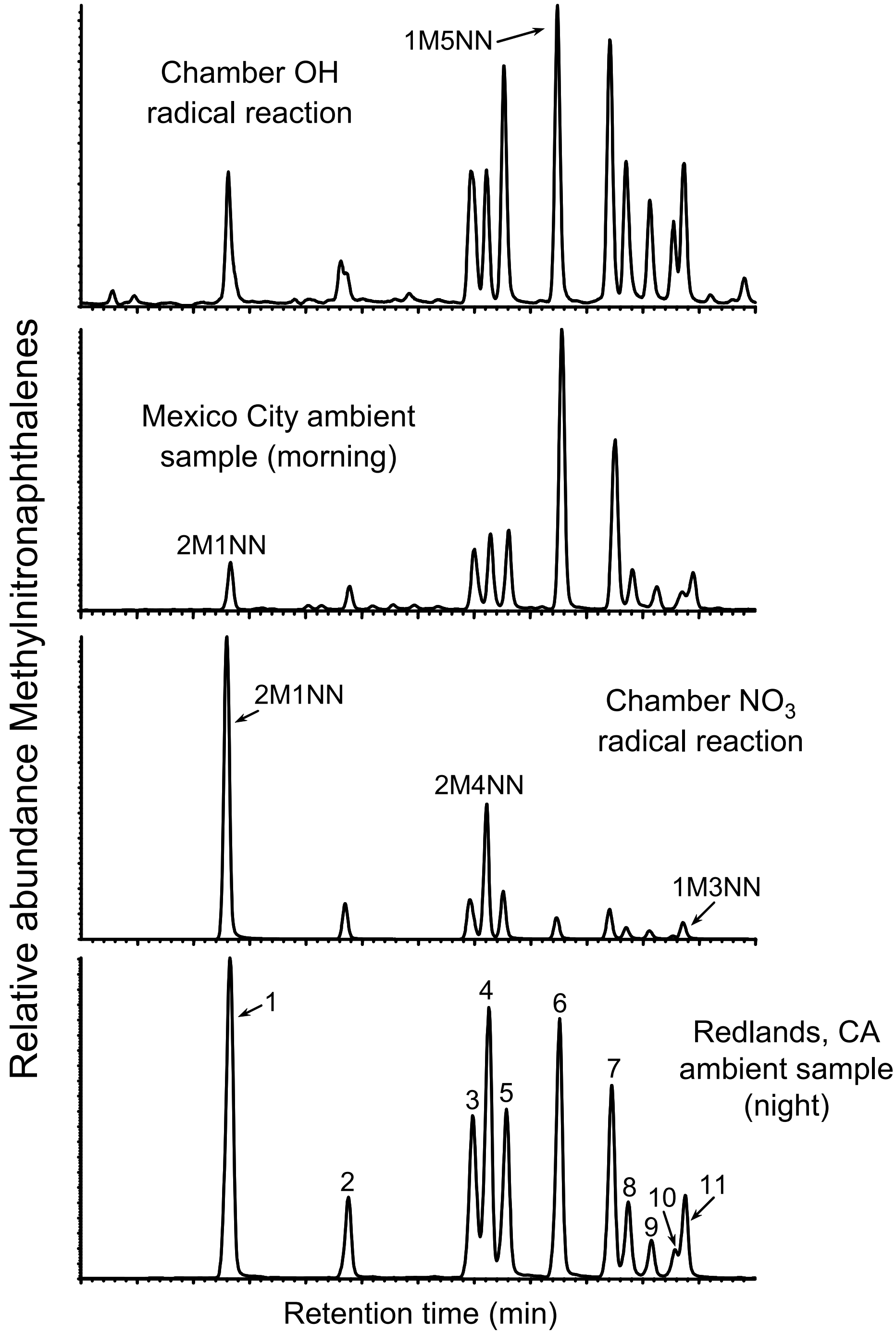

Figure 1. GC-MS NCI analyses, ion chromatograms (187 da) showing the relative abundance of the methylnitronaphthalenes: (top trace) methylnitronaphthalenes (MNNs) formed from a chamber OH radical-initiated reaction of 2-methylnaphthalene (2MN) and 1-methylnaphthalene (1MN); (2^{nd} trace) MNNs present in an ambient sample collected in Mexico City in April, 2003. (3^{rd} trace) MNNs formed from a chamber NO_3 radical-initiated reaction of 2MN and 1MN and (4^{th} trace) MNNs in an ambient sample collected in Redlands, CA in October, 1994. The MNNs in the Redlands sample were identified by Gupta et al. (1996) as: (1) 2M1NN, (2) 1M8NN, (3) 2M8NN, (4) 2M4NN, (5) 1M2NN + 2M5NN, (6) 1M5NN, (7) 1M6NN + 1M4NN, (8) 2M7NN, (9) 2M6NN, (10) 1M7NN, and (11) 1M3NN. The MNNs in the chamber reactions were sampled using Solid Phase MicroExtraction fibers and the ambient samples were collected with modified Hi-Vol samplers with polyurethane foam plugs located down-stream of filters.

al., 1997), and remains to be confirmed. Postulated reactions leading to the formation of phenolic compounds and ring-opened 1,2- and unsaturated 1,4- and 1,6-dicarbonyls are shown in Scheme 2 resulting from the reaction of one of the possible OH-toluene adducts with O_2, based on the studies of Bohn and Zetzsch (1999), Bohn (2001), Klotz et al. (2002) and Volkamer et al. (2001).

Because the measured product formation yields can vary with the NO_2 (and NO) concentration (Atkinson and Aschmann, 1994; Bethel et al., 2000; Klotz et al., 2002), product data for atmospheric purposes can only be obtained from product studies carried out at low NO_x concentrations (parts-per-billion mixing ratios) or from studies in which the NO_2 was varied sufficiently to allow reliable extrapolation to the low NO_2 concentrations representative of atmospheric conditions. Note that the formation yields of the products formed after the H-atom abstraction pathway are independent of NO_2 concentration, at least up to NO_2 mixing ratios of several parts-per-million (see, for example, Bethel et al., 2000).

For benzene, the studies of Volkamer et al. (2001, 2005) show the formation of phenol and glyoxal in 53.1 ± 6.6% and 35.2 ± 9.6% molar yields, respectively. These two products are much more reactive towards reaction with the OH radical than is benzene, by factors of >10, and glyoxal also photolyzes. From its concentration-time behavior, glyoxal was concluded to be a primary product, and the lack of secondary formation of glyoxal allowed an upper limit of ≤8% to be placed on the formation yield of the di-unsaturated 1,6-dicarbonyl HC(O)CH=CHCH=CHCHO at low NO_x concentrations (Volkamer et al., 2001). The yield of HC(O)CH=CHCH=CHCHO increased at high (part-per-million mixing ratio) NO levels (Klotz et al., 2002).

More extensive product data are available for toluene and the xylene isomers. For toluene, the products identified and quantified are (Atkinson and Arey, 2003, and references therein; OEEHA, 2006): benzaldehyde, 6%; benzyl nitrate, 0.8%; *o*-cresol, 12%; *m*-cresol, 2.6%; *p*-cresol, 3%; glyoxal (and C_5-unsaturated 1,4-dicarbonyl co-products), ~30%; and methylglyoxal (plus HC(O)CH=CHCHO co-product), 17%, thereby accounting for ~70% of the reaction products. Table 3 shows the products observed and their formation yields from the *p*-xylene reaction, for which we presently have the most information concerning 1,2-dicarbonyl and unsaturated 1,4-dicarbonyl co-product formation. Again, the time-concentration profiles of glyoxal (Volkamer et al., 2001) and 3-hexene-2,5-dione (Bethel et al., 2000) observed in recent studies show that these dicarbonyls are primary products and that they are not formed to any significant extent from other first-generation products.

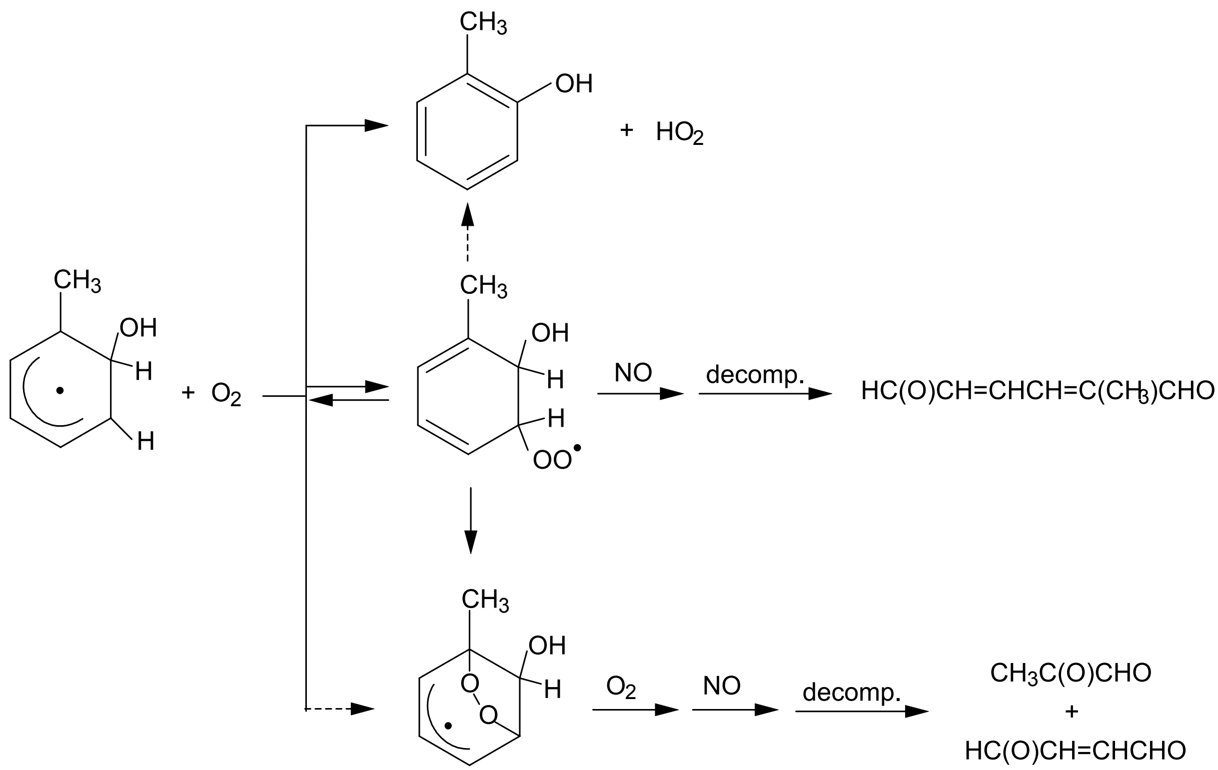
CH3
OH
+ HO2
CH3
OH
H
+ O2
H
CH3
OH
H
H
OO•
NO
decomp.
HC(O)CH=CHCH=C(CH3)CHO
CH3
OH
O
O
H
O2
NO
decomp.
CH3C(O)CHO
+
HC(O)CH=CHCHO

Scheme 2

Table 3. Measured molar product yields from the reaction of *p*-xylene with the OH radical carried out at atmospheric pressure of air, expected to be applicable to atmospheric conditions.

Product	Yield (%)	Reference
p-Methylbenzyl nitrate	0.82 ± 0.16	Atkinson et al. (1991)
p-Tolualdehyde	7.01 ± 1.03 10.3 ± 1.6 7.06 ± 0.42	Atkinson et al. (1991) Smith et al. (1999) Bethel et al. (2000)
2,5-Dimethylphenol	13 ± 1.8 13.8 ± 1.6	Smith et al. (1999) Bethel et al. (2000)
Glyoxal	39.4 ± 11 31.9 ± 5[a]	Smith et al. (1999) Volkamer et al. (2001, 2005)
Methylglyoxal	21.7 ± 7.6	Smith et al. (1999)
3-Hexene-2,5-dione	22.1 ± 4 32.3[b]	Smith et al. (1999) Bethel et al. (2000)
$HC(O)C(CH_3)=CHCHO$	7.1	Smith et al. (1999)

[a]Re-evaluated relative to a yield for *p*-tolualdehyde of 7.0%.
[b]At low NO_2 concentrations.

It therefore appears that the products formed from the H-atom abstraction pathway (typically a few percent) plus phenolic compounds and 1,2-dicarbonyls [plus their co-products which in most cases have not been quantified, although observed by GC-MS after derivatization (Yu et al., 1997) and by *in situ* atmospheric pressure ionization mass spectrometry (Kwok et al., 1997)] account for approximately 70% of the products and reaction pathways. Based on studies with product analyses by GC-MS after derivatization (Yu and Jeffries, 1997; Yu et al., 1997) and by *in situ* atmospheric pressure ionization mass spectrometry (Kwok et al., 1997), the remaining products, at least for the xylene reactions, could include di-unsaturated 1,6-dicarbonyls, unsaturated epoxy-1,6-dicarbonyls, and epoxycyclohexenones. Based on the data of Klotz et al. (2002) for the benzene reaction, where *trans*-, *trans*-2,4-hexadienal has been identified and quantified, di-unsaturated 1,6-dicarbonyls appear to be formed only at high NO concentrations (>0.1 parts-per-million) [see also Scheme 2]. Under conditions representative of the ambient atmosphere, Volkamer et al. (2001) derived a ≤8% yield of $HC(O)CH=CHCH=CHCHO$ from benzene. However, Yu et al. (1997) and Kwok et al. (1997) reported evidence for the formation of di-unsaturated 1,6-dicarbonyls, unsaturated epoxy-1,6-dicarbonyls, and epoxycyclohexenones from the photooxidations of toluene (Yu et al., 1997), xylenes (Yu et al., 1997; Kwok et al., 1997) and trimethylbenzenes (Yu et al., 1997) at NO_x mixing ratios of ≤1 part-per-million.

Clearly, more work is required to identify (in an isomer-specific manner) and quantify unsaturated 1,4-dicarbonyls, di-unsaturated 1,6-dicarbonyls, unsaturated epoxy-1,6-dicarbonyls, and epoxycyclohexenones, and ascertain their formation pathways and yields under atmospheric conditions, as well as any dependence of their yields on NO and NO_2 concentrations.

Unsaturated 1,4-dicarbonyls and di-unsaturated 1,6-dicarbonyls are more reactive than their precursor aromatic hydrocarbon(s) and, as evident from the discussion above, their identification and quantification has proven difficult. These dicarbonyls react with OH radicals, NO_3 radicals and O_3, and also photolyze (Calvert et al., 2002), although the database for their kinetics and products is small (Calvert et al., 2002). Indeed, data are available only for the reactions of OH radicals with *cis*- and *trans*-1,4-butenedial [from the single study of Bierbach et al. (1994)], 4-oxo-2-pentenal [from the single study of Bierbach et al. (1994)], *cis*- and *trans*-3-hexene-2,5-dione, and (with the data for the O_3 reactions being stated to be preliminary) for the reactions of OH radicals, NO_3 radicals and O_3 with *trans*,*trans*- and *cis*,*trans*-2.4-hexadienedial (Klotz et al., 1995, 1999). Apart from 3-hexene-2,5-dione (Calvert et al., 2002), few data (and in most cases no data) are available for the reactions of the ring-opened unsaturated dicarbonyl products of aromatic hydrocarbons.

2. Specific Objective

To identify the ring-opened dicarbonyl and carbonyl products formed from the gas-phase reactions of OH radicals with a series of monocyclic aromatic hydrocarbons under conditions where the OH-aromatic adducts + O_2 reaction was dominant. Specifically, we have used Solid-Phase MicroExtraction (SPME) fibers pre-coated with *O*-(2,3,4,5,6-pentafluorobenzyl)hydroxylamine (PFBHA) for on-fiber derivatization of carbonyl compounds to investigate the carbonyl-containing products formed from the OH radical-initiated reactions of toluene, *o*-, *m*- and *p*-xylene and 1,2,3-, 1,2,4- and 1,3,5-trimethylbenzene.

3. Experimental Methods

Experiments were carried out in a ~7000 liter volume Teflon chamber at 296 ± 2 K and ~735 Torr of dry purified air. The chamber is equipped with two parallel banks of blacklamps for irradiation, and a Teflon-coated fan to ensure rapid mixing of reactants during their introduction into the chamber. Hydroxyl radicals were generated by the photolysis of methyl nitrite in air at wavelengths >300 nm,

$$CH_3ONO + h\nu \rightarrow CH_3O^\bullet + NO$$

$$CH_3O^\bullet + O_2 \rightarrow HCHO + HO_2$$

$$HO_2 + NO \rightarrow OH + NO_2$$

and NO was included in the reactant mixtures to suppress the formation of O_3 and of NO_3 radicals. The initial concentrations of CH_3ONO, NO and aromatic hydrocarbon were ~2.4 x 10^{13} molecule cm^{-3} each, and irradiations were carried out for 3-20 min, resulting in 20-22% (toluene, *o*- and *m*-xylene and 1,2,3-trimethylbenzene) and 30-37% (*p*-xylene and 1,2,4- and 1,3,5-trimethylbenzene) consumption of the initially present aromatic hydrocarbon.

The concentrations of the aromatic hydrocarbons were measured by gas chromatography with flame ionization detection (GC-FID). Gas samples of 100 cm^3 volume were collected from the chamber onto Tenax-TA solid adsorbent with subsequent thermal desorption at ~250 ^oC onto a 30 m DB-5MS megabore column held at –40 ^oC and then temperature programmed to 250 ^oC

at 8 ^oC min^{-1}. The carbonyl products were analyzed by combined gas chromatography-mass spectrometry using on-fiber derivatization with SPME (Reisen et al., 2005) and employing a 65 μm polydimethylsiloxane/divinylbenzene PDMS/DVB fiber. The fibers were coated with PFBHA by a 30 min headspace extraction over a vigorously stirred aqueous solution of PFBHA hydrochloride. The PFBHA coating of the fiber was carried out under nitrogen gas to minimize any acetone contamination from laboratory air. The coated fiber was then exposed to the reactants in the chamber for 5 min, with the chamber mixing fan on, to form a carbonyl oxime (Martos and Pawliszyn, 1998). For the GC-MS analyses, the exposed fiber was then removed from the chamber and thermally desorbed in the injection port of a Varian 2000 GC/MS/MS at 250 °C onto a 30 m DB-1701 megabore column held at 40 ^oC and then temperature programmed at 8 ^oC min^{-1} to 260 ^oC, with isobutane chemical ionization.

The NO and initial NO_2 concentrations were measured using a Thermo Environmental Instruments, Inc., Model 42 chemiluminescent NO-NO_2-NO_x analyzer, noting that for these NO-NO_x instruments, CH_3ONO contributes ~100% to the "NO_2" signal. The estimated NO_2 concentrations at the end of the irradiation [assuming that ([NO] + [NO_2]) remained constant during the irradiations (Atkinson et al., 1989)] were in the range (1.0-2.1) x 10^{13} molecule cm^{-3} (0.4-0.9 parts-per-million mixing ratio). The chemicals used, and their stated purity, were: benzaldehyde (98%), 2,3-butanedione (99%), *O*-(2,3,4,5,6-pentafluorobenzyl)hydroxylamine hydrochloride (98+%), *m*-tolualdehyde (97%, *p*-tolualdehyde (97%), toluene (99+%), 1,2,3-trimethylbenzene, 1,2,4-trimethylbenzene, 1,3,5-trimethylbenzene (98%), *o*-xylene (97%), *m*-xylene (99+%) and *p*-xylene (99+%), Aldrich Chemical Company; *o*-tolualdehyde, Pfalz and Bauer; and NO (≥99.0%), Matheson Gas Products. Methyl nitrite was synthesized as decribed by Taylor et al. (1980) and stored at 77 K under vacuum.

4. Results

A series of CH_3ONO – NO – aromatic hydrocarbon – air irradiations were carried out, with analysis of the aromatic hydrocarbon by Tenax/GC-FID and analysis of carbonyl-containing compounds after on-fiber derivation with subsequent GC-MS analyses. From the GC-MS analyses of the exposed SPME fibers, we observed mono- and/or di-derivatives of a series of dicarbonyls seen as $[M+H]^+$ and $[M+41]^+$ adduct ions [where M is the molecular weight of the mono-derivatized (where derivatization to form the oxime has added 195 mass units) or di-derivatized (where derivatization to form the di-oxime has added 390 mass units) dicarbonyl]. Glyoxal [$(CHO)_2$], methylglyoxal [$CH_3C(O)CHO$], biacetyl [$CH_3C(O)C(O)CH_3$] and 3-hexene-2,5-dione [$CH_3C(O)CH{=}CHC(O)CH_3$] were identified based on comparison with standards analyzed by GC-MS using the same sampling and analysis procedures. The standards were either commercially available (biacetyl), synthesized in-house (3-hexene-2,5-dione) or generated *in situ* from reactions in which they are known to be formed. Thus, glyoxal was generated from the OH radical-initiated reaction of 3-methyl-2-butenal (see B. 2-1. below) and methylglyoxal was generated from the OH radical-initiated reaction of methacrolein (Tuazon and Atkinson, 1990). Although we lacked authentic standards for comparison, several additional dicarbonyls were formed from two or more of the aromatic hydrocarbons, thereby allowing their structures to be proposed.

Representative total ion chromatograms (TICs) are shown in Figure 2-8 for toluene, *o*-, *m*- and *p*-xylene and 1,2,3-, 1,2,4- and 1,3,5-trimethylbenzene, respectively. The carbonyl-containing products are noted on the figures.

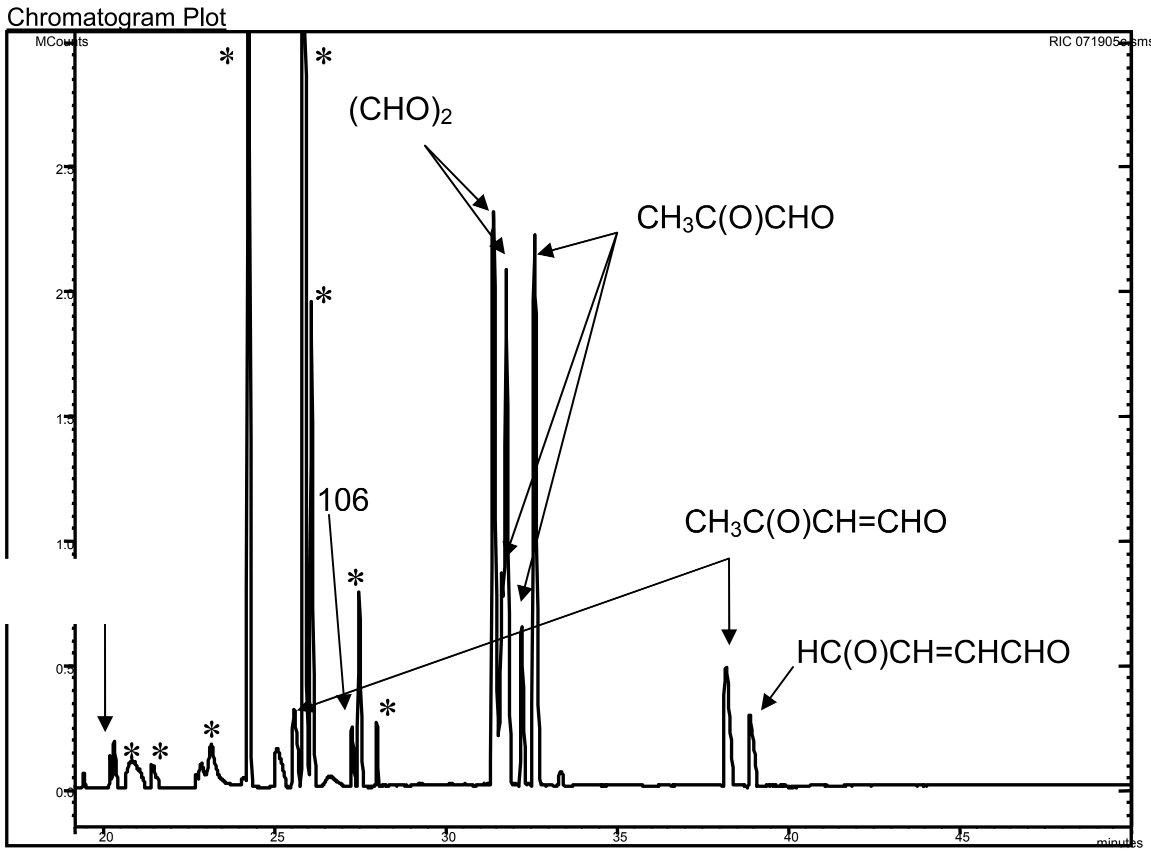

Figure 2. GC-MS total ion trace of an OH + toluene reaction (22% toluene reacted). The peak labeled "106" is the oxime of benzaldehyde, formed after H-atom abstraction from the CH_3 group. The (*) indicates peaks that were either present in the pre-reaction sample or were due to the derivitization reagent. Note that dicarbonyls may appear as either mono-oximes, di-oximes or both. The mono-oximes elute prior to 30 min and the di-oximes after 30 min.

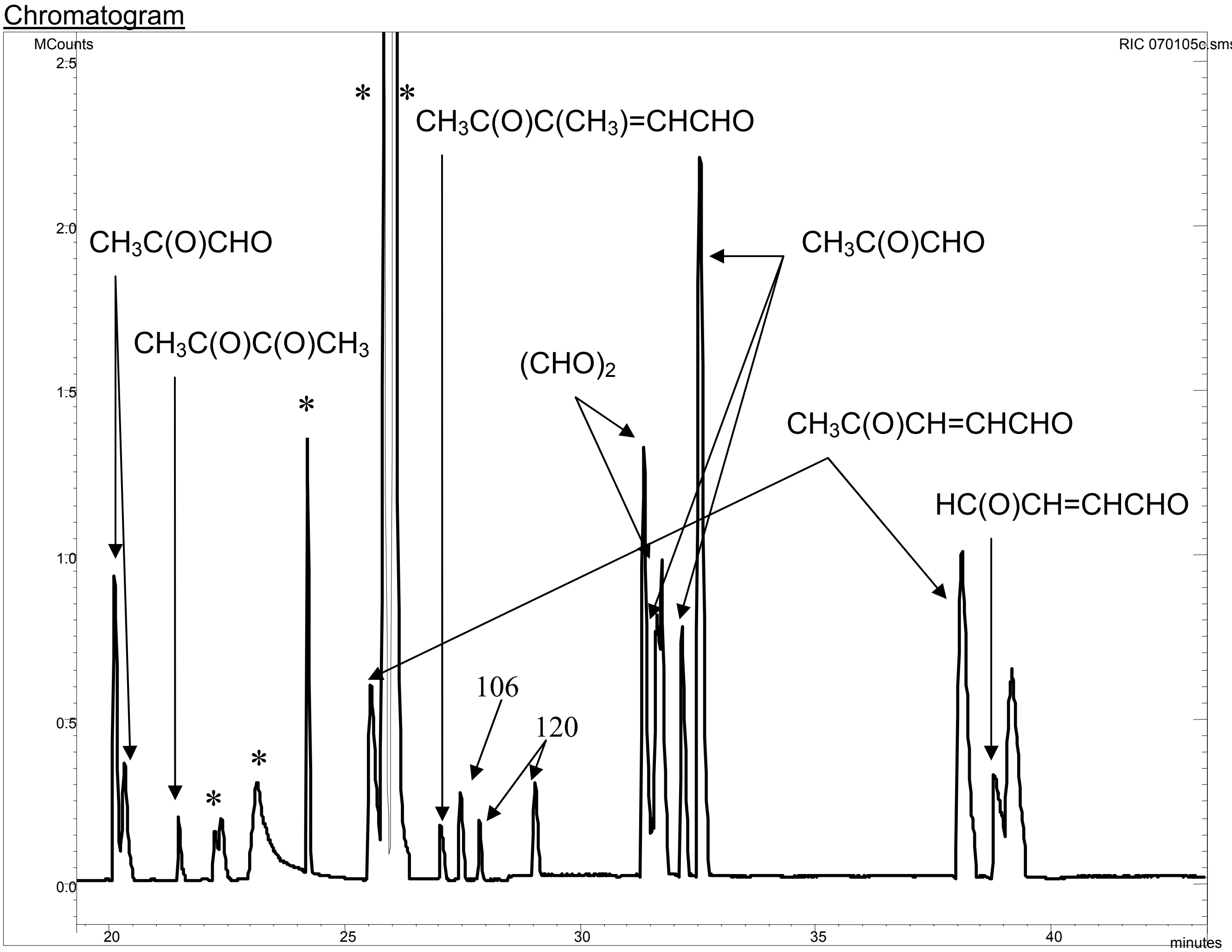

Figure 3. GC-MS total ion trace of an OH + *o*-xylene reaction (20% *o*-xylene reacted). The peaks labeled "106" and "120" are the oximes of benzaldehyde and of *o*-tolualdehyde, respectively. The (*) indicates peaks that were either present in the pre-reaction sample or were due to the derivitization reagent. Note that dicarbonyls may appear as either mono-oximes, di-oximes or both. The mono-oximes elute prior to 30 min and the di-oximes after 30 min.

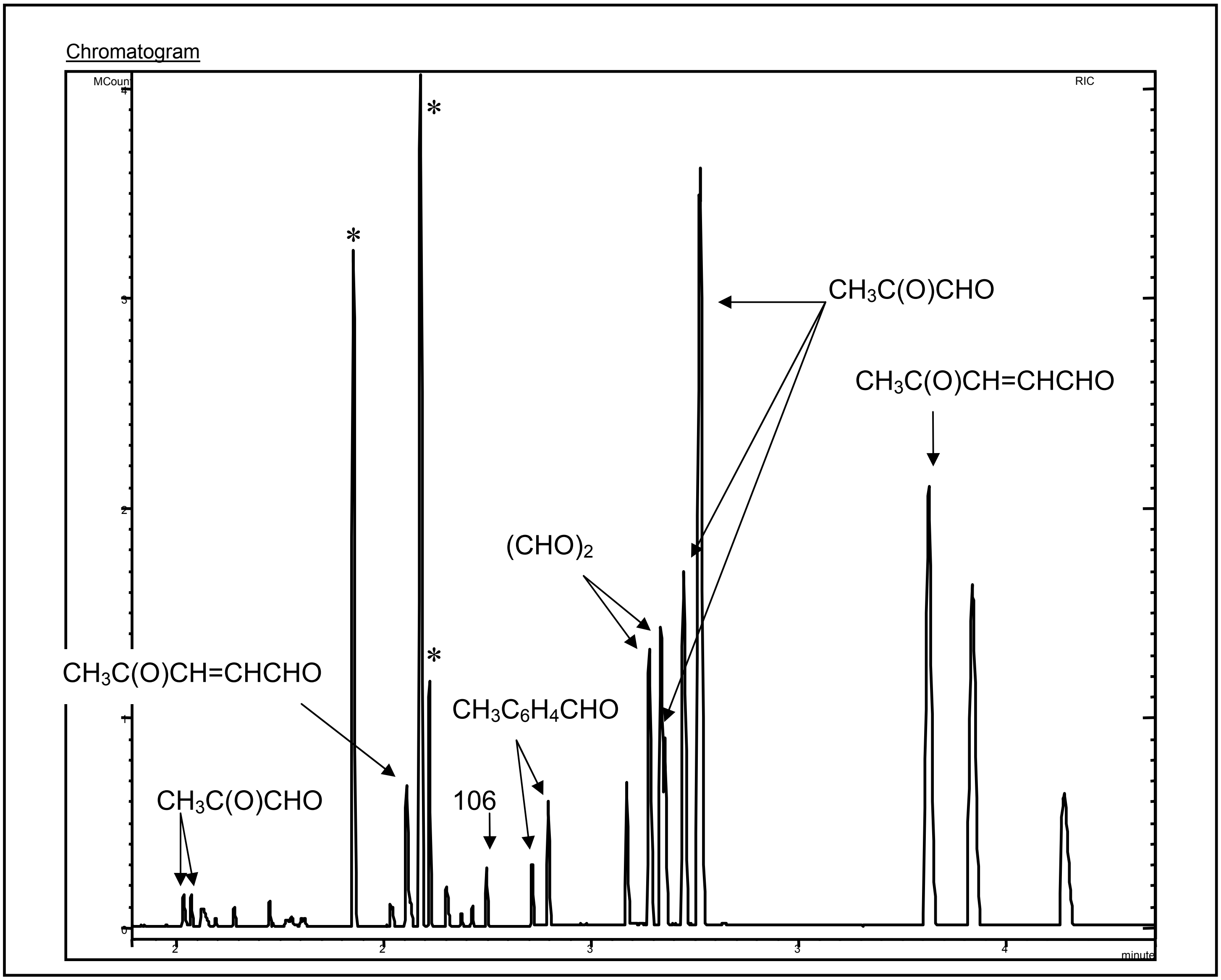

Figure 4. GC-MS total ion trace of an OH + *m*-xylene reaction (20% *m*-xylene reacted). The peak labeled "106" is benzaldehyde and $CH_3C_6H_4CHO$ is *m*-tolualdehyde. The (*) indicates peaks that were either present in the pre-reaction sample or were due to the derivitization reagent. Note that dicarbonyls may appear as either mono-oximes, di-oximes or both. The mono-oximes elute prior to 30 min and the di-oximes after 30 min.

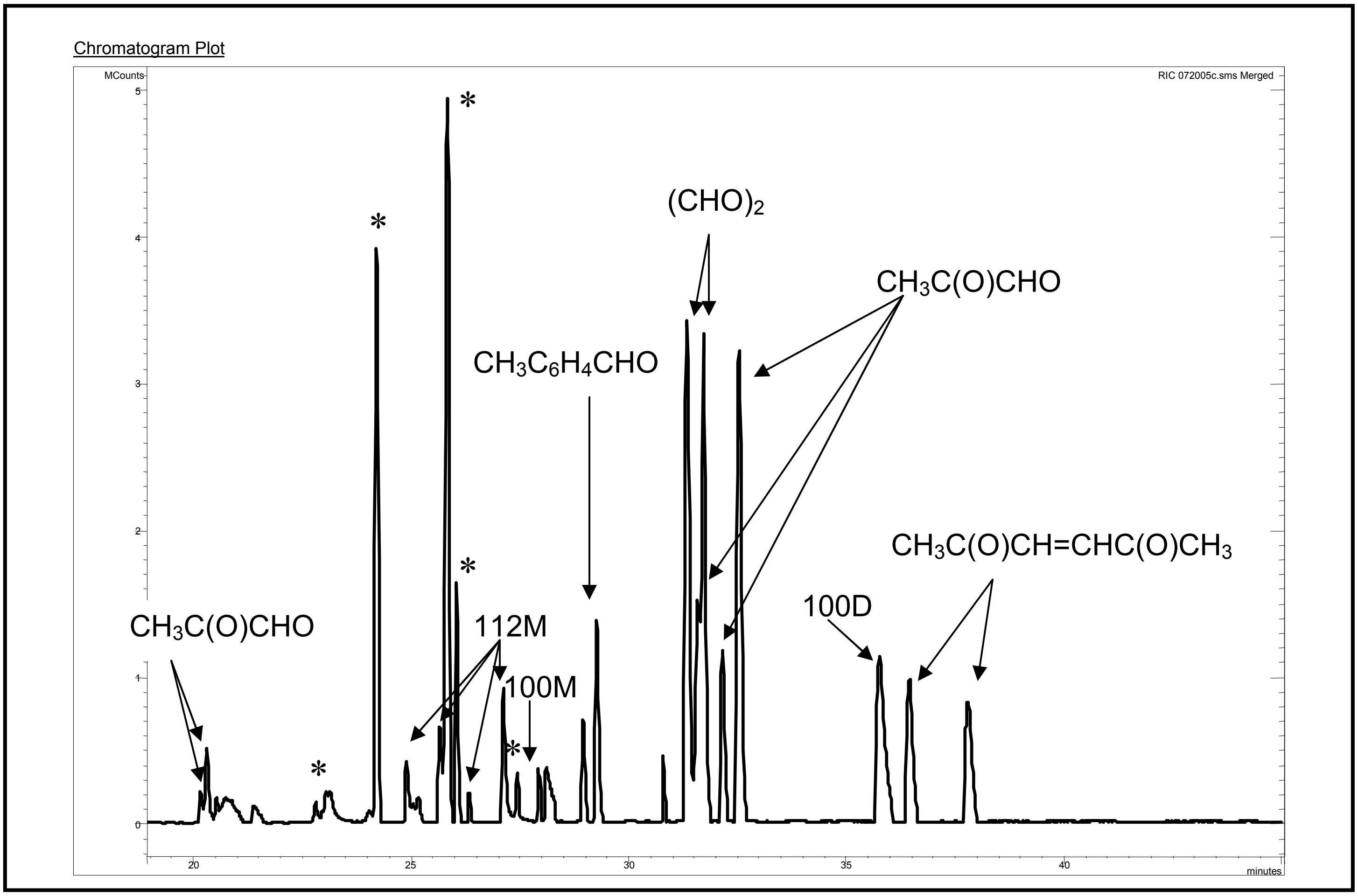

Figure 5. GC-MS total ion trace of an OH + *p*-xylene reaction (33% *p*-xylene reacted). The peaks labeled "112M" are the mono-oxime derivatives of $CH_3C(O)CH{=}CHC(O)CH_3$. The peaks labeled "100M" and "100D" are a dicarbonyl of molecular weight 100 present as its mono- (100M) and di- (100D) oxime derivatives. $CH_3C_6H_4CHO$ is *p*-tolualdehyde. The (*) indicates peaks that were either present in the pre-reaction sample or were due to the derivitization reagent. Note that dicarbonyls may appear as either mono-oximes, di-oximes or both. The mono-oximes elute prior to 30 min and the di-oximes after 30 min.

•Chromatogram

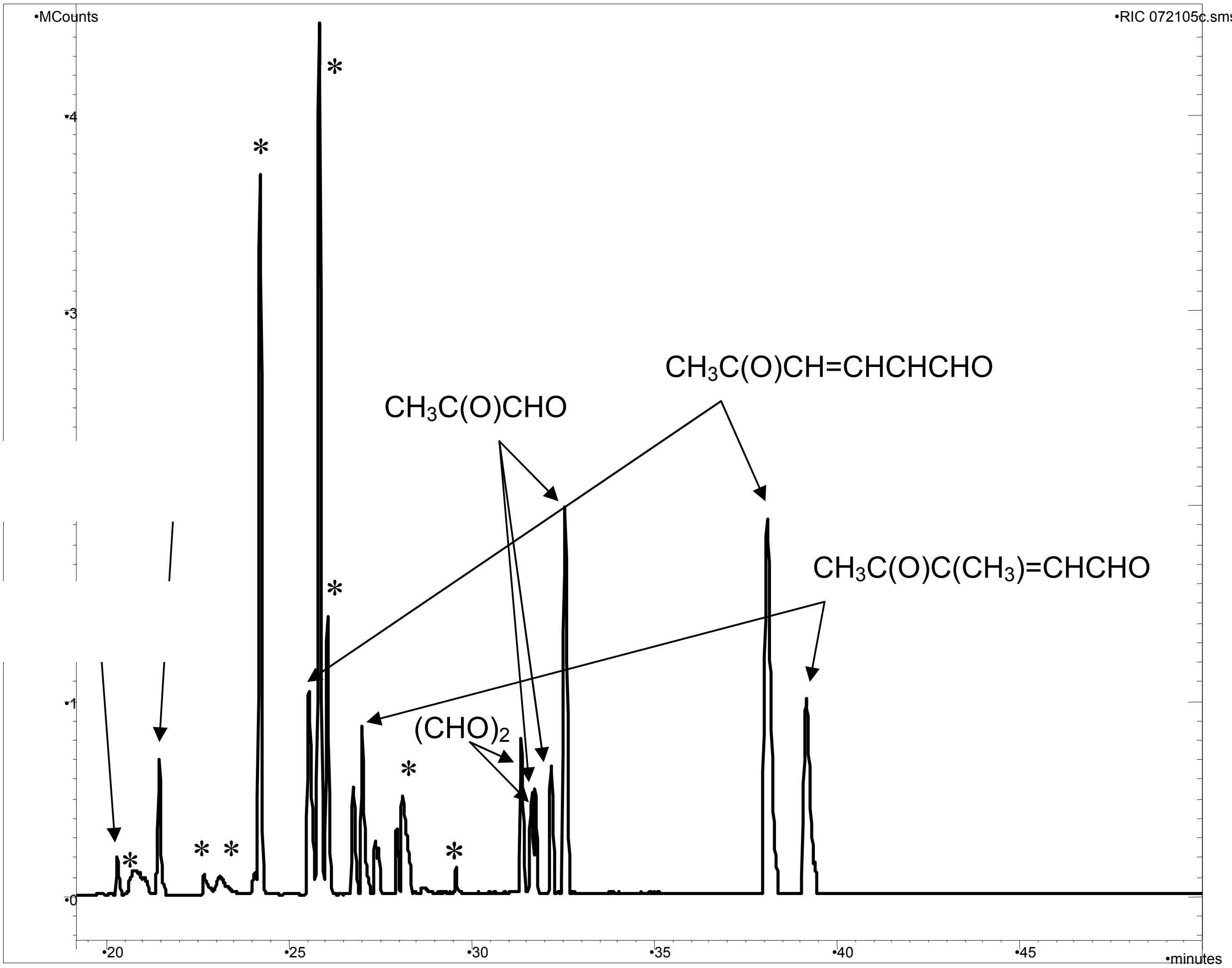

Figure 6. GC-MS total ion trace of an OH + 1,2,3-trimethylbenzene reaction (22% 1,2,3-trimethylbenzene reacted). The (*) indicates peaks that were either present in the pre-reaction sample or were due to the derivitization reagent. Note that dicarbonyls may appear as either mono-oximes, di-oximes or both. The mono-oximes elute prior to 30 min and the di-oximes after 30 min.

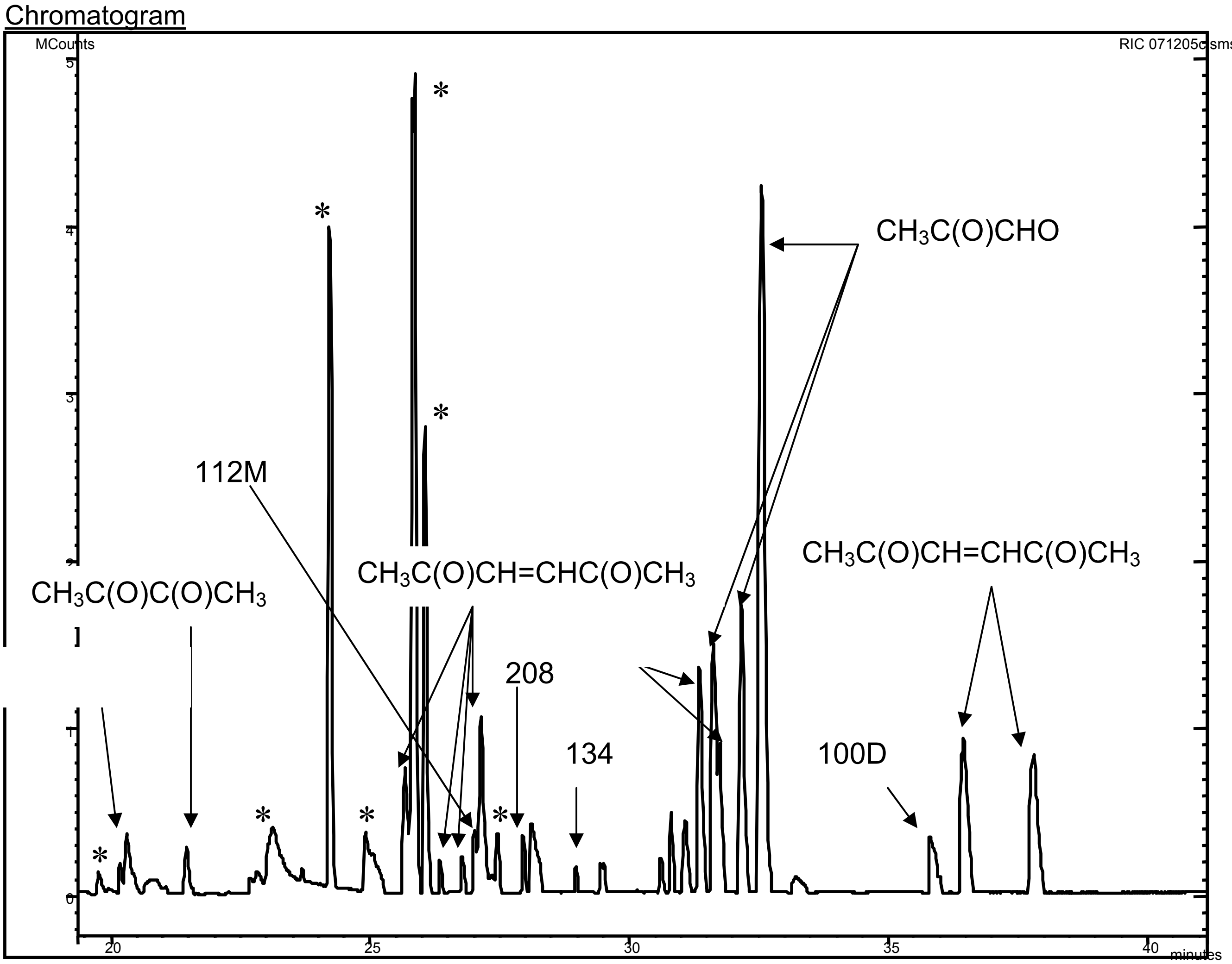

Figure 7. GC-MS total ion trace of an OH + 1,2,4-trimethylbenzene reaction (37% 1,2,4-trimethylbenzene reacted). The peak labeled "112M" is a mono-oxime of $CH_3C(O)C(CH_3)=CHCHO$, that labeled "134" is a dimethylbenzaldehyde, and that labeled "100D" is a di-oxime of a molecular weight 100 dicarbonyl. The (*) indicates peaks that were either present in the pre-reaction sample or were due to the derivitization reagent. Note that dicarbonyls may appear as either mono-oximes, di-oximes or both. The mono-oximes elute prior to 30 min and the di-oximes after 30 min.

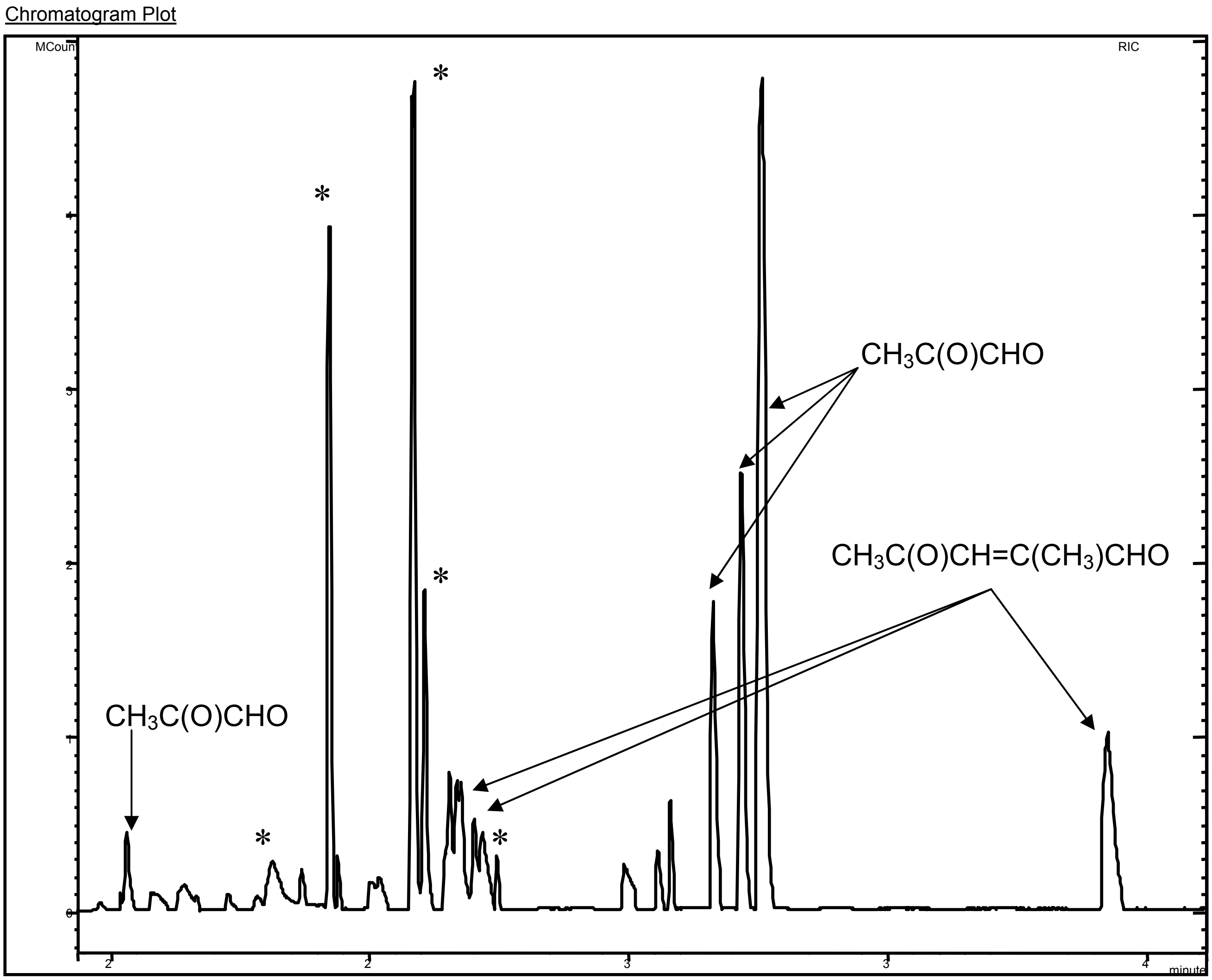

Figure 8. GC-MS total ion trace of an OH + 1,3,5-trimethylbenzene reaction (30% 1,3,5-trimethylbenzene reacted). The (*) indicates peaks that were either present in the pre-reaction sample or were due to the derivitization reagent. Note that dicarbonyls may appear as either mono-oximes, di-oximes or both. The mono-oximes elute prior to 30 min and the di-oximes after 30 min.

Table 4. Ring-opened dicarbonyls observed and their assignments

	toluene	xylene			trimethylbenzene		
ring-opened product		*o*-	*m*-	*p*-	1,2,3-	1,2,4-	1,3,5-
$(CHO)_2$	•	•	•	•	•	•	
$CH_3C(O)CHO$	•	•	•	•	•	•	•
$CH_3C(O)C(O)CH_3$		•			•	•	
HC(O)CH=CHCHO	•	•					
$CH_3C(O)CH{=}CHCHO$	•	•	•		•		
$HC(O)C(CH_3){=}CHCHO$							
$CH_3C(O)C(CH_3){=}CHCHO$		•			•	•	
$CH_3C(O)CH{=}CHC(O)CH_3$				•		•	
$CH_3C(O)CH{=}C(CH_3)CHO$							•
$HC(O)C(CH_3){=}C(CH_3)CHO$							

We can attribute the majority of the peaks observed to mono- and/or di-oximes of the 1,2-dicarbonyls glyoxal, methylglyoxal and biacetyl, and a series of unsaturated 1,4-dicarbonyls shown or attributed to be due to 2-butenedial [HC(O)CH=CHCHO], $CH_3C(O)CH{=}CHCHO$, $CH_3C(O)CH{=}CHC(O)CH_3$, $CH_3C(O)C(CH_3){=}CHCHO$ and $CH_3C(O)CH{=}C(CH_3)CHO$. In addition, oximes of benzaldehyde (molecular weight 106) and *o*-, *m*- and *p*-tolualdehyde (molecular weight 120) were also observed from toluene and the xylenes (resulting from the initial H-atom abstraction pathway). The small "doublet" peak after the mono-oximes of methylglyoxal is due to a contaminant carbonyl of molecular weight 86 (possibly 2-pentanone) present in the derivatizing agent, and the peak labeled 106 in the xylene reactions is benzaldehyde, presumably due to some carry over from previous experiments. Based on our understanding of the reaction mechanism, and taking the *o*-xylene reaction as the example, the *o*-tolualdehyde arises after initial H-atom abstraction, while the remaining products observed from the *o*-xylene reaction arise after initial OH radical addition to the aromatic ring, these being: $(CHO)_2$ + $CH_3C(O)C(CH_3){=}CHCHO$, $CH_3C(O)CHO$ + $CH_3C(O)CH{=}CHCHO$ and $CH_3C(O)C(O)CH_3$ + HC(O)CH=CHCHO.

We see no evidence for the formation of the following classes of previously postulated and/or qualitatively observed (Kwok et al., 1997; Yu et al., 1997) [see below for structures]:

- Di-unsaturated 1,6-dicarbonyls such as $CH_3C(O)CH{=}CHCH{=}CHCHO$ and its isomers and homologs (of molecular weight 124 from toluene, 138 from the xylenes and 152 from the trimethylbenzenes.

- Unsaturated epoxy-1,6-dicarbonyls.
- Epoxycyclohexenones.

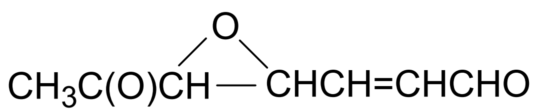

unsaturated epoxy-1,6-dicarbonyl

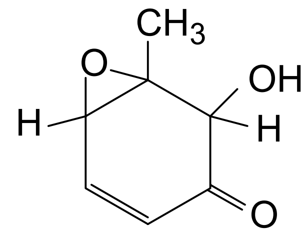

epoxycyclohexenone

Assuming that the sets of 1,2-dicarbonyl + unsaturated 1,4-dicarbonyl products arise after reaction schemes such as that shown in Scheme 2, then the following sets of co-products can potentially be formed.

Toluene

$(CHO)_2$ + $CH_3C(O)CH{=}CHCHO$
$(CHO)_2$ + *$HC(O)C(CH_3){=}CHCHO$*
$CH_3C(O)CHO$ + $HC(O)CH{=}CHCHO$

***o*-Xylene**

$(CHO)_2$ + $CH_3C(O)C(CH_3){=}CHCHO$
$(CHO)_2$ + *$HC(O)C(CH_3){=}C(CH_3)CHO$*
$CH_3C(O)CHO$ + $CH_3C(O)CH{=}CHCHO$
$CH_3C(O)C(O)CH_3$ + $HC(O)CH{=}CHCHO$

***m*-Xylene**

$(CHO)_2$ + *$CH_3C(O)CH{=}C(CH_3)CHO$*
$CH_3C(O)CHO$ + *$HC(O)C(CH_3){=}CHCHO$*
$CH_3C(O)CHO$ + $CH_3C(O)CH{=}CHCHO$

***p*-Xylene**

$(CHO)_2$ + $CH_3C(O)CH{=}CHC(O)CH_3$
$CH_3C(O)CHO$ + *$HC(O)C(CH_3){=}CHCHO$*

1,2,3-Trimethylbenzene

$(CHO)_2$ + *$CH_3C(O)C(CH_3){=}C(CH_3)CHO$*
$CH_3C(O)CHO$ + $CH_3C(O)C(CH_3){=}CHCHO$
$CH_3C(O)C(O)CH_3$ + $CH_3C(O)CH{=}CHCHO$

1,2,4-Trimethylbenzene

$(CHO)_2$ + *$CH_3C(O)C(CH_3)=CHC(O)CH_3$*
$CH_3C(O)CHO$ + *$HC(O)C(CH_3)=C(CH_3)CHO$*
$CH_3C(O)CHO$ + *$CH_3C(O)CH=C(CH_3)CHO$*
$CH_3C(O)CHO + CH_3C(O)C(CH_3)=CHCHO$
$CH_3C(O)CHO + CH_3C(O)CH=CHC(O)CH_3$
$CH_3C(O)C(O)CH_3$ + *$HC(O)C(CH_3)=CHCHO$*

1,3,5-Trimethylbenzene

$CH_3C(O)CHO + CH_3C(O)CH=C(CH_3)CHO$

Our data are in general agreement with this expectation, with the products not observed being in italics. This non-observation could be due to (a) low detection sensitivity of our on-fiber derivatization method for these specific compounds, or (b) a low formation yield of them such that their concentration is too low during the experiments for us to detect them, or (c) they are formed but undergo rapid isomerization or other loss process. The fact that we do not observe the presence of $HC(O)C(CH_3)=CHCHO$ from any of the reactions which could form it (toluene, m-xylene and 1,2,4-trimethylbenzene), of $HC(O)C(CH_3)=C(CH_3)CHO$ from either of the reactions which could form it (*o*-xylene and 1,2,4-trimethylbenzene), of $CH_3C(O)CH=C(CH_3)CHO$ from either of the reactions which could form it (*m*-xylene and 1,2,4-trimethylbenzene), or of the two C_9-unsaturated 1,4-dicarbonyls $CH_3C(O)C(CH_3)=C(CH_3)CHO$ and $CH_3C(O)C(CH_3)=CHC(O)CH_3$ suggests that it is an analytical problem and/or that these specific compounds undergo a rapid loss mechanism.

5. Conclusions

Our data to date show that the ring-opened products are glyoxal + co-products, methylglyoxal + co-products and 2,3-butanedione + co-products, with 2,3-butanedione only being formed from *o*-xylene and 1,2,3- and 1,2,4-trimethylbenzene. The co-products are unsaturated 1,4-dicarbonyls, although not all possible unsaturated 1,4-dicarbonyls are observed. The dicarbonyl product assignments to date are listed in Table 4; as mentioned above, benzaldaldehyde, tolualdehydes and a dimethylbenzaldehyde are also observed in the toluene, xylene and 1,2,4-trimethylbenzene reactions, respectively, and are formed after H-atom abstraction from the C-H bonds of the methyl substituent group(s).

B. Mechanisms of the Gas-Phase Reactions of OH Radicals with Naphthalene and Alkyl-Naphthalenes

1. Introduction

As noted in the general Introduction, there are no published data on the absolute or relative rate constants of the reactions of OH-PAH adducts with O_2 and NO_2. The observation of nitro-PAH characteristic of OH radical-initiated reactions of PAH in the presence of NO_x in ambient air samples from urban air (Arey et al., 1987, 1989; Zielinska et al., 1989; Arey, 1998; Arey and Atkinson, 2003; Reisen and Arey, 2005) suggests that the OH-PAH adducts react with

NO_2 to a significant extent in polluted urban airmasses. Further evidence for this conclusion arises from experiments carried out by Atkinson et al. (1994) in which the reaction of NO_3 radicals with naphthalene was investigated as a function of NO_2 and O_2 concentrations. An upper limit to the rate constant ratio of $k_{O2}/k_{NO2} <4 \times 10^{-7}$ was obtained at 298 ± 2 K, corresponding to the reaction of the NO_3-naphthalene adduct with NO_2 dominating over the reaction with O_2 down to at least 80 ppbv of NO_2 (and possibly much lower) in the atmosphere.

Assuming that the daytime nitronaphthalene and methylnitronaphthalene concentrations in the atmosphere are governed by gas-phase formation from the OH radical reaction (with yield α) and loss by photolysis (Arey et al., 1990),

$$\text{OH + naphthalene} \rightarrow \alpha \text{ nitronaphthalene} \qquad (k_{OH})$$

$$\text{nitronaphthalene} \rightarrow \text{products} \qquad (k_{phot})$$

then

$$[\text{nitronaphthalene}] = \alpha\, k_{OH}\, [\text{OH}]\, [\text{naphthalene}]/k_{phot} \qquad \text{(I)}$$

For 1-nitronaphthalene the lifetime due to photolysis has been estimated to be 24 min (Phousongphouang and Arey, 2003b), while the photolysis lifetime of 2-nitronaphthalene was estimated to be 177 min (Phousongphouang and Arey, 2003b). Therefore, Eq (I) should be appropriate for calculating 1-nitronaphthalene formation yields from ambient data, while losses due to dilution will introduce greater uncertainty in the predicted formation yields of the longer-lived 2-nitronaphthalene. Table 5 gives ambient concentration data for naphthalene and nitronaphthalenes taken in southern California covering nearly a 20-year time span, and also includes recent data from Mexico City (Arey et al., 2004).

Using these ambient concentration data and Eq (I), the predicted 1- and 2-nitronaphthalene formation yields (α) for the OH + naphthalene reaction under atmospheric conditions can be calculated from the measured ratios of [nitronaphthalene]/[naphthalene], the literature values of $k_{OH} = 2.4 \times 10^{-11}$ cm^3 molecule^{-1} s^{-1} (see Table 1), $k_{phot} = 6.8 \times 10^{-4}$ s^{-1} for 1-nitronaphthalene and 9.5×10^{-5}s^{-1} for 2-nitronaphthalene at an estimated 12-hr average light intensity (Phousongphouang and Arey, 2003b) and estimated average OH radical concentrations of (1-5) x 10^6 molecule cm^{-3} (the lowest OH concentration being applied to the Riverside wintertime samples). Daytime or mid-day samples were chosen to minimize carry-over from nighttime NO_3 radical-initiated reactions (which in recent studies (Reisen and Arey, 2005) have been suggested to be important even in locations previously thought of as "source areas"). The calculated formation yields of 1-nitronaphthalene are 0.5-2% and of 2-nitronaphthalene are 0.1-0.4%. These nitronaphthalene formation yields derived from ambient measurements are consistent with laboratory chamber reactions conducted under high-NO_x conditions, in which formation yields of 1-nitronaphthalene of 0.32 ± 0.28% (Atkinson et al., 1987) and 1.2 ± 0.9% (Sasaki et al., 1997) and of 2-nitronaphthalene of 0.27 ± 0.34% (Atkinson et al., 1987) and 1.3 ± 1.1% (Sasaki et al., 1997) were reported. Although the reported laboratory yields of 1- and 2-nitronaphthalene are close to 1:1 (Atkinson et al., 1987; Sasaki et al., 1997), ambient data

Table 5. Ambient concentration data and predicted formation yields of 1-nitronaphthalene (1-NN) and 2-nitronaphthalene (2-NN).

Location, date and local sampling times	Naphthalene ($ng\ m^{-3}$)	1-NN ($pg\ m^{-3}$)	2-NN ($pg\ m^{-3}$)	[OH] (radical cm^{-3})	1-NN formation yield (%)	2-NN formation yield (%)
Torrance, CA[a]						
Feb. 25, 1986 (0600-1800)	3300	3000	2900	5×10^6	0.52	0.07
Glendora, CA[b]						
Aug. 13, 1986 (0800-2000)	2400	2300	1800	2×10^6	1.36	0.15
Aug. 15-18, 1986 (0800-2000)	3025	2400	2400	2×10^6	1.12	0.16
Aug. 20, 1986 (0800-2000)	4100	2700	2600	2×10^6	0.93	0.13
Los Angeles, CA[c]						
Aug. 12-16, 2002 (1100-1430)	152	243	243	5×10^6	0.91	0.13
Riverside, CA[c]						
Aug. 26-30, 2002 (1100-1430)	54.8	201	273	5×10^6	2.08	0.39
Los Angeles, CA[c]						
Jan. 13-17, 2003 (1100-1430)	758	132	144	1×10^6	0.49	0.08
Riverside, CA[c]						
Jan. 27-31, 2003 (1100-1430)	110	41	53	1×10^6	1.06	0.19
Mexico City, Mexico[d]						
April 27, 2003 (1100-1600)	107	195	175	5×10^6	1.03	0.13
April 28, 2003 (1100-1600)	290	285	331	5×10^6	0.56	0.09
April 29, 2003 (1100-1600)	371	409	514	5×10^6	0.62	0.11
April 30, 2003 (1100-1600)	195	360	314	5×10^6	1.05	0.13

[a]Data from Arey et al. (1987). A high [OH] is used because very high HONO concentrations were measured at this site (Winer et al., 1987).
[b]Naphthalene and nitronaphthalene concentration data and estimated value for [OH] from Arey et al. (1989).
[c]Naphthalene and nitronaphthalene concentration data from Reisen and Arey (2005). OH radical concentrations assumed.
[d]Unpublished data for naphthalene, 1-NN and 2-NN. The concentration of OH radicals estimated based on measurements during MCMA 2003 (Arey et al., 2004).

suggest that the formation yield of 2-NN is less than that of 1-NN. This apparent discrepancy between ambient and laboratory data could be due to a greater importance of dilution relative to photolysis for 2-NN. Indeed, we previously derived a dilution rate of (3.4–5.9) x 10^{-5} s^{-1} for nighttime periods during the 1986 study in Glendora, CA (Arey et al., 1989), this being of a similar magnitude to the photolysis rate of 2-NN. It is clear that ambient atmospheric nitronaphthalene data are consistent with the 1- and 2-nitronaphthalene formation yields measured in the laboratory at part-per-million mixing ratios of NO_2, which have large uncertainties associated with them due to the low formation yields. This general consistency of ambient data with laboratory product data suggests that the OH-PAH adducts react to a significant extent with NO_2 even under ambient urban atmospheric conditions.

2. Objectives

To determine the effect of NO_2 concentration on selected products formed from the OH radical-initiated reaction of naphthalene. Among the products previously observed from naphthalene (Sasaki et al., 1997; Reisen, 2003), we have chosen to look at glyoxal and nitronaphthalenes, and this necessitated three specific sub-tasks:

- Since generation of glyoxal from the commercially available glyoxal hydrate is a difficult and time-consuming endeavor (Tuazon and Atkinson, 1989), an *in situ* method of generating a quantitative amount of glyoxal was needed.

- Investigation of the formation yield of glyoxal from OH + naphthalene as a function of NO_x concentration.

- Preliminary studies to investigate the formation yield of nitronaphthalenes from OH + naphthalene and of other nitroaromatics from the OH radical-initiated reactions of their parent aromatic, as a function of NO_x concentration.

2-1. ***In Situ*** Glyoxal Calibration: Kinetics and Products of the OH Radical-Initiated Reaction of 3-Methyl-2-butenal

The gas-phase reactions of α,β-unsaturated carbonyls such as acrolein [CH_2=CHCHO], crotonaldehyde [*trans*-CH_3CH=CHCHO], methacrolein [CH_2=C(CH_3)CHO] and methyl vinyl ketone [CH_3C(O)CH=CH_2] result in formation of glyoxal from acrolein and crotonaldehyde, with measured yields of 5 ± 2% from acrolein (Magneron et al., 2002) and of 16 ± 4% (Magneron et al., 2002) and 21 ± 5% (Orlando and Tyndall, 2002) from crotonaldehyde, and of methylglyoxal from methacrolein in 8.4 ± 1.6% yield (Tuazon and Atkinson, 1990). In this work we have extended these previous studies of acrolein, crotonaldehyde and methacrolein by investigating the kinetics and products of the reaction of 3-methyl-2-butenal [$(CH_3)_2$C=CHCHO] with OH radicals, with a goal of using the OH radical-initiated reaction of 3-methyl-2-butenal as a routine *in situ* quantitative source of glyoxal for calibration of Solid Phase MicroExtraction fibers using on-fiber derivatization.

2-1.1. Experimental Methods

Most experiments were carried out at 296 ± 2 K and 740 Torr total pressure of purified air at ~5% relative humidity in two ~7000 liter volume Teflon chambers, each equipped with two parallel banks of blacklamps for irradiation and a Teflon-coated fan to ensure rapid mixing of reactants during their introduction into the chamber. Experiments utilizing *in situ* Fourier transform infrared (FT-IR) spectroscopy were carried out at 298 ± 2 K and 740 Torr total pressure of synthetic air (80% N_2 + 20% O_2) in a 5870 liter Teflon-coated, evacuable chamber equipped with a multiple reflection optical system interfaced to a Mattson Galaxy 5020 FT-IR spectrometer. Irradiation was provided by a 24-kW xenon arc lamp, with the light being filtered through a 6 mm thick Pyrex pane to remove wavelengths <300 nm. IR spectra were recorded with 32 scans per spectrum (corresponding to a 1.2 min averaging time) at a full-width-at-half-maximum resolution of 0.7 cm^{-1} and a pathlength of 62.9 or 36.8 m. Hydroxyl radicals were generated in the presence of NO by the photolysis of methyl nitrite in air at wavelengths >300 nm, and NO was added to the reactant mixtures to suppress the formation of O_3 and hence of NO_3 radicals [see (A)above].

Kinetic Studies. The rate constant for the reaction of OH radicals with 3-methyl-2-butenal was measured using a relative rate method, in which the relative decay rates of 3-methyl-2-butenal and a reference compound, whose OH radical reaction rate constant is reliably known, were measured in the presence of OH radicals. Providing that 3-methyl-2-butenal and the reference compound (methacrolein in this case) were removed only by reaction with OH radicals, then,

$$\ln\left(\frac{[\text{3-methyl-2-butenal}]_{to}}{[\text{3-methyl-2-butenal}]_t}\right) = \frac{k_1}{k_2}\ln\left(\frac{[\text{methacrolein}]_{to}}{[\text{methacrolein}]_t}\right) \qquad \text{(II)}$$

where [3-methyl-2-butenal]$_{to}$ and [methacrolein]$_{to}$ are the concentrations of 3-methyl-2-butenal and methacrolein at time t_o, respectively, [3-methyl-2-butenal]$_t$ and [methacrolein]$_t$ are the corresponding concentrations at time t, and k_1 and k_2 are the rate constants for reactions (1) and (2), respectively.

(1) OH + 3-methyl-2-butenal → products

(2) OH + methacrolein → products

Hence a plot of ln([3-methyl-2-butenal]$_{to}$/[3-methyl-2-butenal]$_t$) against ln([methacrolein]$_{to}$/[methacrolein]$_t$) should be a straight line of slope k_1/k_2 and zero intercept.

A series of CH_3ONO – NO – 3-methyl-2-butenal – methacrolein – air irradiations were carried out, with initial concentrations (molecule cm^{-3}) of: CH_3ONO, ~2.4 x 10^{14}; NO, ~2.4 x 10^{14}; and 3-methyl-2-butenal and methacrolein, ~2.4 x 10^{13} each. Irradiations were carried out at 20% of the maximum light intensity for 2-8 min. 3-Methyl-2-butenal and methacrolein were analyzed by GC-FID, with gas samples of 100 cm^3 volume being collected from the chamber onto Tenax-TA solid adsorbent with subsequent thermal desorption at ~250 ^oC onto a 30 m DB-1701 megabore column, initially held at -40 ^oC and then temperature programmed to 200 ^oC at 8 ^oC min^{-1}.

Product Analyses by *in situ* FT-IR Spectroscopy. For the experiments conducted in the evacuable chamber with *in situ* FT-IR analyses, the initial reactant concentrations (in molecule cm^{-3}) were: CH_3ONO, 2.46 x 10^{14}; NO, 2.46 x 10^{14}; and 3-methyl-2-butenal, 1.23 x 10^{14} and 1.70 x 10^{14}, carried out with 62.9 m and 36.8 m pathlengths, respectively. The two experiments involved intermittent irradiation (1-4 min duration each) with IR spectra being recorded during the dark periods and with total irradiation times of 17.5-18.5 min. Calibration IR spectra of 3-methyl-2-butenal and glyoxal were measured by introducing measured partial pressures of 3-methyl-2-butenal and glyoxal into the evacuable chamber and recording the IR spectra. A compilation of calibration spectra, including those of acetone and methyl nitrite and its phooxidation products, using the present FT-IR spectrometer and the same spectral parameters as used here was available from previous studies.

Product Analyses by SPME/GC-FID and SPME/GC-MS. The formation yield of 2-hydroxy-2-methylpropanal [$(CH_3)_2C(OH)CHO$], an anticipated product which does not elute from GC columns without prior derivatization (Reisen et al., 2003; Baker et al., 2004), was determined by Solid Phase MicroExtraction (SPME) using on-fiber derivatization (Reisen et al., 2003; Baker et al., 2004). As described previously (Reisen et al., 2003; Baker et al., 2004), 2-hydroxy-2-methylpropanal was sampled using a 65 μm poly(dimethylsiloxane)/divinylbenzene (PDMS/DVB) “StableFlex” SPME fiber which was coated prior to use with *O*-(2,3,4,5,6-pentafluorobenzyl)hydroxylamine (PFBHA) for on-fiber derivatization of carbonyl compounds. The derivatization reagent was loaded onto the SPME fiber for 30 min using headspace extraction from a ~20 mg ml^{-1} PFBHA hydrochloride solution immediately before sampling in the chamber. The coated fiber was inserted into the chamber and exposed to the chamber contents for 5 minutes with the chamber mixing fan on. The fiber was then removed and introduced into the injection port of the GC-FID held at 250 ^oC for thermal desorption onto a 30 m DB-1701 megabore column held at 40 ^oC and then temperature programmed to 260 ^oC at 8 ^oC min^{-1}. Product identification was by combined gas chromatography-mass spectrometry (GC-MS), using a Varian 2000 MS/MS with isobutane chemical ionization and equipped with a DB-1701 column.

2-Hydroxy-2-methylpropanal is not commercially available, and therefore the amount of 2-hydroxy-2-methylpropanal formed from the OH radical-initiated reaction of 3-methyl-2-butenal was compared to that formed from the OH radical-initiated reaction of 2-methyl-3-buten-2-ol, where the formation yield of 2-hydroxy-2-methylpropanal has been measured to be 31 ± 4% (Reisen et al., 2003). From three series of sequential CH_3ONO – NO – 3-methyl-2-butenal – air and CH_3ONO – NO – 2-methyl-3-buten-2-ol – air irradiations, the 2-hydroxy-2-methylpropanal formation yield from 3-methyl-2-butenal was obtained from the expression,

$$\text{Yield} = \left(\frac{[\text{2H2MP}]_{\text{3-methyl-2-butenal}}}{[\text{2H2MP}]_{\text{2-methyl-3-buten-2-ol}}}\right) \text{X} \left(\frac{F_{\text{3-methyl-2-butenal}}}{F_{\text{2-methyl-3-buten-2-ol}}}\right)$$

$$\text{X} \left(\frac{[\text{2-methyl-3-buten-2-ol] reacted}}{[\text{3-methyl-2-butenal] reacted}}\right) \text{X} \ (31 \pm 4)\% \qquad \text{(III)}$$

where $[2H2MP]_{3\text{-methyl-2-butenal}}$ and $[2H2MP]_{2\text{-methyl-3-buten-2-ol}}$ are the measured concentrations of 2-hydroxy-2-methylpropanal formed from the reactions of OH radicals with 3-methyl-2-butenal and 2-methyl-3-buten-2-ol, respectively, $F_{3\text{-methyl-2-butenal}}$ and $F_{2\text{-methyl-3-buten-2-ol}}$ are the multiplicative correction factors (1.08-1.12 for these experiments) to correct the measured 2-hydroxy-2-methylpropanal concentrations for secondary reaction with OH radicals,[28] and ([2-methyl-3-buten-2-ol] reacted) and ([3-methyl-2-butenal] reacted) are the amounts of 2-methyl-3-buten-2-ol and 3-methyl-2-butenal reacted, respectively. The concentrations of 3-methyl-2-butenal and 2-methyl-3-buten-2-ol were measured by GC-FID after sample collection onto Tenax-TA solid adsorbent, as described above.

The initial concentrations (molecule cm^{-3}) were: CH_3ONO, ~(1.2-2.4) x 10^{13}; NO, ~(1.2-2.4) x 10^{13}; and 3-methyl-2-butenal or 2-methyl-3-buten-2-ol, (1.46-3.08) x 10^{13}, with the initial CH_3ONO, NO and 3-methyl-2-butenal (or 2-methyl-3-buten-2-ol) concentrations being approximately equal. Irradiations were carried out at 20% of the maximum light intensity for 5 min, resulting in 49-58% consumption of the initial 3-methyl-2-butenal or 2-methyl-3-buten-2-ol (3-methyl-2-butenal and 2-methyl-3-buten-2-ol are almost identically reactive towards the OH radical [this work and IUPAC, 2006]).

NO concentrations and the initial NO_2 concentration were measured during the experiments by a Thermo Environmental Instruments Inc. Model 42 chemiluminescence NO-NO_2-NO_x analyzer (note that CH_3ONO is measured as "NO_2" by commercial NO-NO_2-NO_x analyzers).

The chemicals used, and their stated purities, were: 3-methyl-2-butenal (97%), 2-methyl-3-buten-2-ol (98%), *O*-(2,3,4,5,6-pentafluorobenyl)hydroxylamine hydrochloride (98+%) and methacrolein (95%), Aldrich Chemical Company; and NO (≥99.0%), Matheson Gas Products. Methyl nitrite was prepared as described by Taylor *et al*. (1980) and stored at 77 K under vacuum. Glyoxal was prepared by heating glyoxal trimeric dihydrate (≥97%, Sigma) in a round-bottomed flask fitted with a distillation column loosely packed with alternating layers of glass wool and P_2O_5. Vapors passing through the column were condensed in a trap at liquid nitrogen temperature (this process taking ~1-2 hr), with occasional pumping to remove non-condensables (probably CO). The trap was then immersed in a dry-ice/acetone bath from which more volatile impurities, such as CO_2, were pumped away, until the pressure reading stabilized at <0.1 Torr. IR spectra of the vapor at room temperature were recorded in a 10 cm pathlength cell and in the evacuable chamber (see above) and checked for consistency of absorbance *versus* partial pressure.

2-1.2. Results

Kinetics. The data obtained from a series of CH_3ONO – NO – 3-methyl-2-butenal – methacrolein – air irradiations are plotted in accordance with Equation (II) in Figure 9. A least-squares analysis of the data leads to a rate constant ratio of $k_1/k_2 = 2.15 \pm 0.06$, where the indicated error is two least-squares standard deviations. This rate constant ratio can be placed on an absolute basis by use of a rate constant for the reaction of OH radicals with methacrolein of $k_2 = 2.89 \times 10^{-11}$ cm^3 $molecule^{-1}$ s^{-1} at 296 K (Atkinson and Arey, 2003; IUPAC, 2006, leading to

$$k_1 = (6.21 \pm 0.18) \times 10^{-11} \text{ cm}^3 \text{ molecule}^{-1} \text{ s}^{-1} \text{ at } 296 \pm 2 \text{ K},$$

where the indicated error is two standard deviations and does not include the uncertainty in the rate constant k_2 (which is expected to be ~±10%). Inclusion of this likely ±10% uncertainty in the rate constant k_2 leads to a rate constant k_1 of

$$k_1 = (6.21 \pm 0.65) \times 10^{-11} \text{ cm}^3 \text{ molecule}^{-1} \text{ s}^{-1} \text{ at } 296 \pm 2 \text{ K}.$$

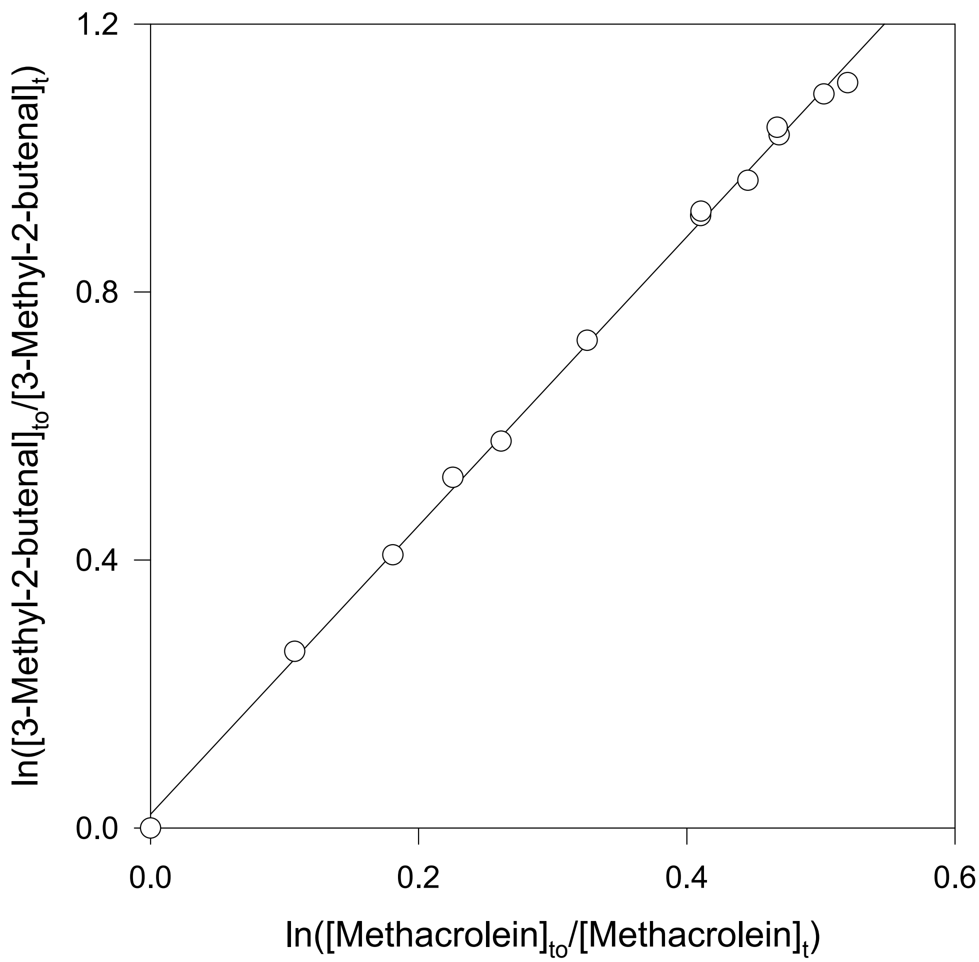

Figure 9. Plot of Equation (II) for the reaction of OH radicals with 3-methyl-2-butenal, with methacrolein as the reference compound. Analyses were by GC-FID.

Product Analyses by *in situ* FT-IR Spectroscopy. Two irradiations of CH_3ONO – NO – 3-methyl-2-butenal – air mixtures were carried out, with quantitative analysis of products and reactants by FT-IR spectroscopy being carried out by a subtractive procedure. Components were successively subtracted from the spectrum of the mixture using calibrated spectra of the gaseous reactants and known products, which have been recorded previously with the same instrument and identical spectral parameters (see Experimental Methods above). Figure 10A shows a spectrum of the initial 1.23×10^{14} molecule cm^{-3} of 3-methyl-2-butenal employed in one experiment and Figure 10B shows the spectrum of the products formed after 60% consumption of the initially present 3-methyl-2-butenal. Spectrum (B) was obtained by subtracting the absorption bands of the unreacted 3-methyl-2-butenal and those of CH_3ONO and NO and their irradiation products NO_2, HCHO, HC(O)OH, CH_3ONO_2, HNO_3, and HONO from the spectrum of the irradiated mixture. Readily identified major products were CO_2, glyoxal and acetone, with the reference spectra of glyoxal and acetone being shown in Figure 10D and Figure 10E, respectively. The familiar, well-resolved absorption band of CO_2 at 2350 cm^{-1} (and of CO at 2145 cm^{-1}) is outside the range of the plots. The residual spectrum (Figure 10C) was obtained by subtraction of the absorptions by glyoxal and acetone from Figure 10B.

Glyoxal and acetone also react with OH radicals (Atkinson and Arey, 2003; IUPAC, 2006), and their measured concentrations were corrected for the OH radical reactions as described previously (Atkinson et al., 1982). The correction factors to take into account secondary reaction with OH radicals depend on the rate constant ratio k(OH + product)/k(OH + 3-methyl-2-butenal) and increase with this rate constant ratio and with the extent of reaction (Atkinson et al., 1982). The corrections were calculated using our measured rate constant for 3-methyl-2-butenal and rate constants at 298 K for the reactions of OH radicals with glyoxal and acetone of 1.1×10^{-11} cm^3 $molecule^{-1}$ s^{-1} and 1.7×10^{-13} cm^3 $molecule^{-1}$ s^{-1}, respectively (Atkinson and Arey, 2003; IUPAC, 2006). The multiplicative correction factors F were <1.10 for glyoxal and <1.002 for acetone (and hence no corrections were made to the measured acetone concentrations). Figure 11 shows plots of the amounts of glyoxal (corrected for secondary reaction with OH radicals) and acetone formed against the amounts of 3-methyl-2-butenal reacted. Least-squares analyses of the data shown in Figure 11 lead to the formation yields given in Table 6.

The residual spectrum of Figure 10C can mostly be attributed to absorptions by peroxyacyl nitrate(s) ($RC(O)OONO_2$) and organic nitrate(s) ($RONO_2$), which are predicted as minor photooxidation products of 3-methyl-2-butenal (see below). The characteristic absorption frequencies of $RC(O)OONO_2$ at 1814, 1737, 1300 and 794 cm^{-1} and those of $RONO_2$ at 1660, 1300 and 850 cm^{-1} are noted in Figure 10C. The aggregate concentrations of the organic nitrate, $RONO_2$, products have been calculated from the area of the 1670 cm^{-1} band[31] using an average integrated absorption coefficient of 2.5×10^{-17} cm $molecule^{-1}$, derived from the corresponding absorption bands of a series of organic nitrates, and have an estimated uncertainty of ±25%. The formation yield of the $RONO_2$ product(s) was independent of the extent of reaction (Figure 11), and the organic nitrate formation yield is reported in Table 6. Because of a lack of data

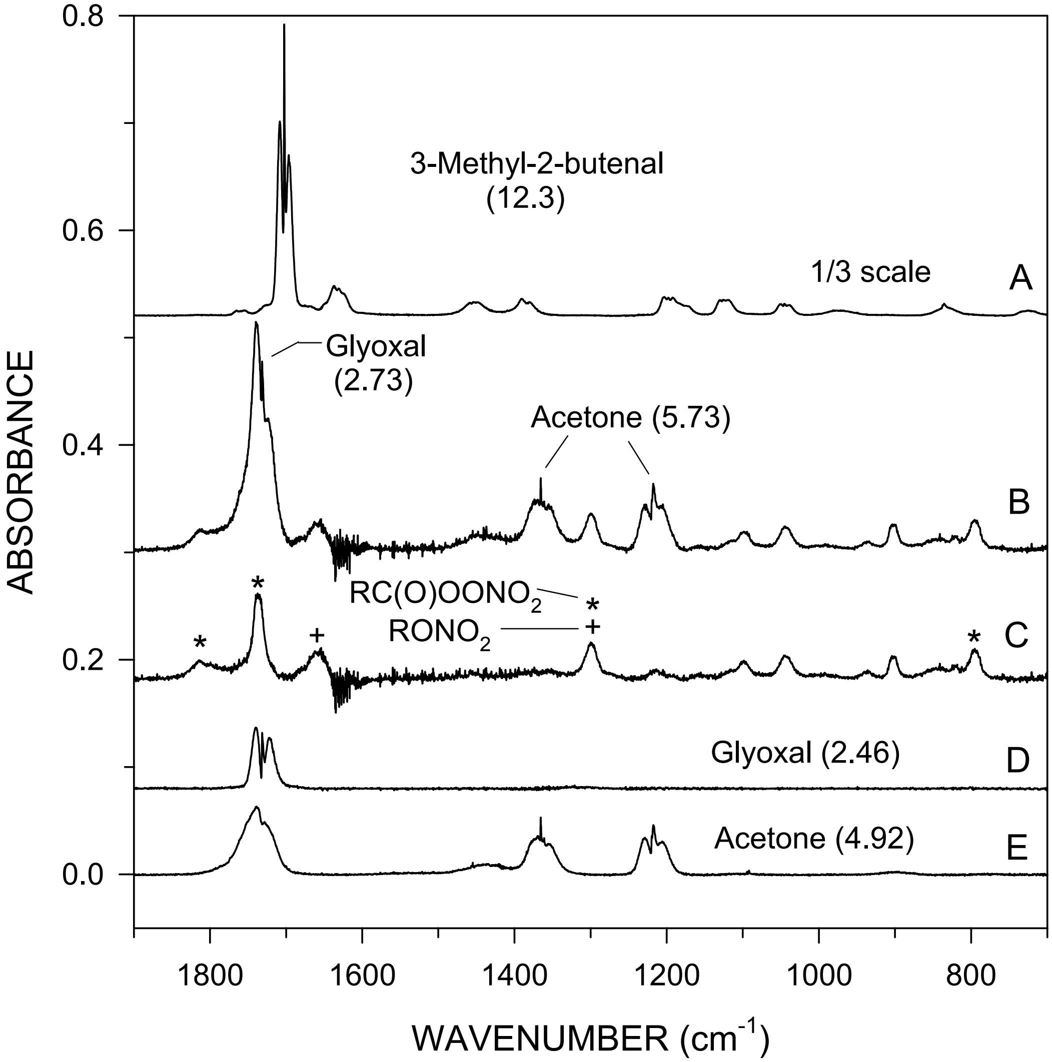

Figure 10. Infrared spectra from a CH_3ONO – NO - 3-methyl-2-butenal – air irradiation. (A) Initial 3-methyl-2-butenal. (B) Products formed from 3-methyl-2-butenal, after 60% consumption of the initially present 3-methyl-2-butenal. (C) From (B) after subtraction of absorptions by the major products acetone and glyoxal, showing the presence of an organic nitrate (+) and a peroxyacyl nitrate (*) as minor products (see text). (D) Reference spectrum of glyoxal. (E) Reference spectrum of acetone. The upper spectral plots are shifted for clarity. Numbers in parentheses are concentrations in units of 10^{13} molecule cm^{-3}. Pathlength = 62.9 m.

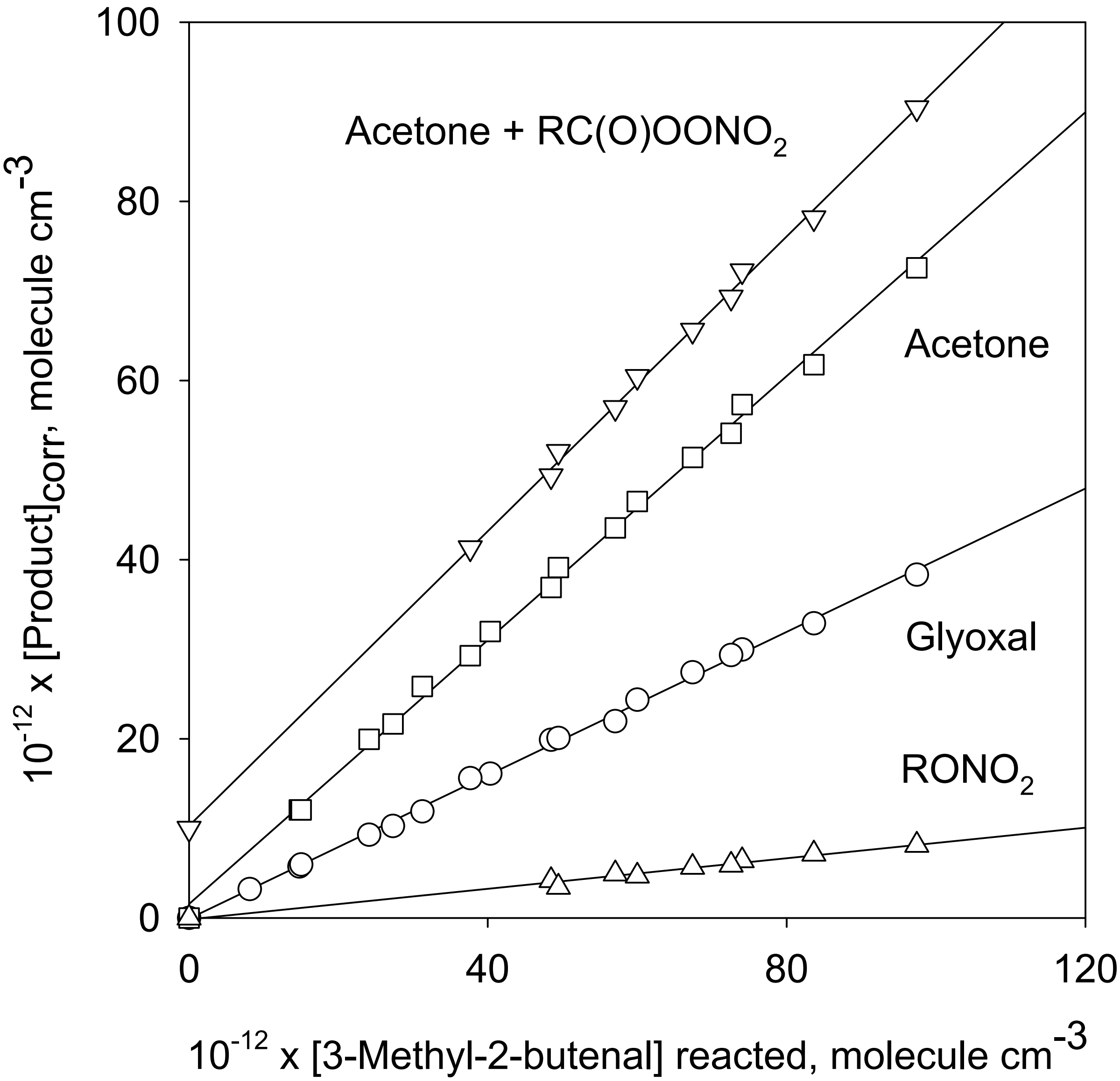

Figure 11. Plots of the amounts of glyoxal, acetone, organic nitrates ($RONO_2$), and of the sum of the amounts of acetone and peroxyacyl nitrate(s) ($RC(O)OONO_2$) formed against the amounts of 3-methyl-2-butenal reacted with OH radicals. The glyoxal data have been corrected for secondary reactions (see text). The (acetone + $RC(O)OONO_2$) data have been displaced vertically by 1.0×10^{13} molecule cm^{-3} for clarity. Analyses were by *in situ* FT-IR spectroscopy.

Table 6. Products observed, and their formation yields, from the OH radical-initiated reaction of 3-methyl-2-butenal in the presence of NO

product	molar formation yield (%)	analysis method
acetone	74 ± 6^a	FT-IR
glyoxal	40 ± 3^a	FT-IR
2-hydroxy-2-methylpropanal	4.6 ± 0.7^b	SPME/GC-FID
CO_2	$39\text{-}30^c$	FT-IR
$RC(O)OONO_2$	$5\text{-}8^d$	FT-IR
$RONO_2$	8.5 ± 2.3^a	FT-IR
$CO_2 + RC(O)OONO_2$	38 ± 6^a	
acetone + $RC(O)OONO_2$	82 ± 8^a	

[a]Indicated errors are two least-squares standard deviations combined with estimated uncertainties in the analysis of: 3-methyl-2-butenal, ±5%; acetone, ±5%; glyoxal, ±5%; CO_2, ±7%; $RC(O)OONO_2$, ±30%; and $RONO_2$, ±25%.
[b]Indicated error is two least-squares standard deviations combined with estimated uncertainties in the GC-FID response factors for 3-methyl-2-butenal and 2-methyl-3-buten-2-ol of ±5% each and in the 2-hydroxy-2-methylpropanal yield from 2-methyl-3-buten-2-ol of ±13% (Reisen et al., 2003).
[c]The yield of CO_2 decreased with reaction time (Figure 12).
[d]The yield of $RC(O)OONO_2$ increased with reaction time (Figure 12).

concerning the reactivity of these organic nitrate(s), attributed to hydroxynitrates (see below), no corrections for secondary reactions were made to the measured concentrations; the predicted hydroxynitrates are expected to be less reactive than the parent 3-methyl-2-butenal and hence corrections for secondary reactions would probably be fairly minor.

The 1737 cm^{-1} band of $RC(O)OONO_2$, like the 1670 cm^{-1} band of $RONO_2$, is due to the asymmetric stretching of the $-NO_2$ group, and the above integrated absorption coefficient can also be applied for estimating the $RC(O)OONO_2$ concentration since our measured absorption coefficients for peroxyacetyl nitrate, peroxypropionyl nitrate and peroxybenzoyl nitrate are within 10% of the above value. However, the 1737 cm^{-1} band seen in Figure 10C still has interferences from the 2-hydroxy-2-methylpropanal product detected by SPME/GC-MS and from the $RONO_2$ products, since the latter are predicted to be multifunctional species (see below) containing hydroxyl and carbonyl groups. Hence, estimates of the $RC(O)OONO_2$ concentration was made on the basis of its weaker but unique absorption band at 1814 cm^{-1}, using an integrated absorption coefficient of 1.1×10^{-17} cm $molecule^{-1}$ which is the average of values measured from the corresponding bands of (in units of 10^{-17} cm $molecule^{-1}$): peroxyacetyl nitrate 1.13; peroxypropionyl nitrate, 0.89; and peroxybenzoyl nitrate, 1.15. The individual $RC(O)OONO_2$ determinations have an estimated ±30% uncertainty. The measured yield of $RC(O)OONO_2$ ranged from 5-8%, with the yield increasing slowly with irradiation time (i.e., with extent of reaction), as shown in Figure 12. While the predicted $RC(O)OONO_2$ product, $(CH_3)_2C{=}CHC(O)OONO_2$ (see below), still contains a C=C bond and may be of similar

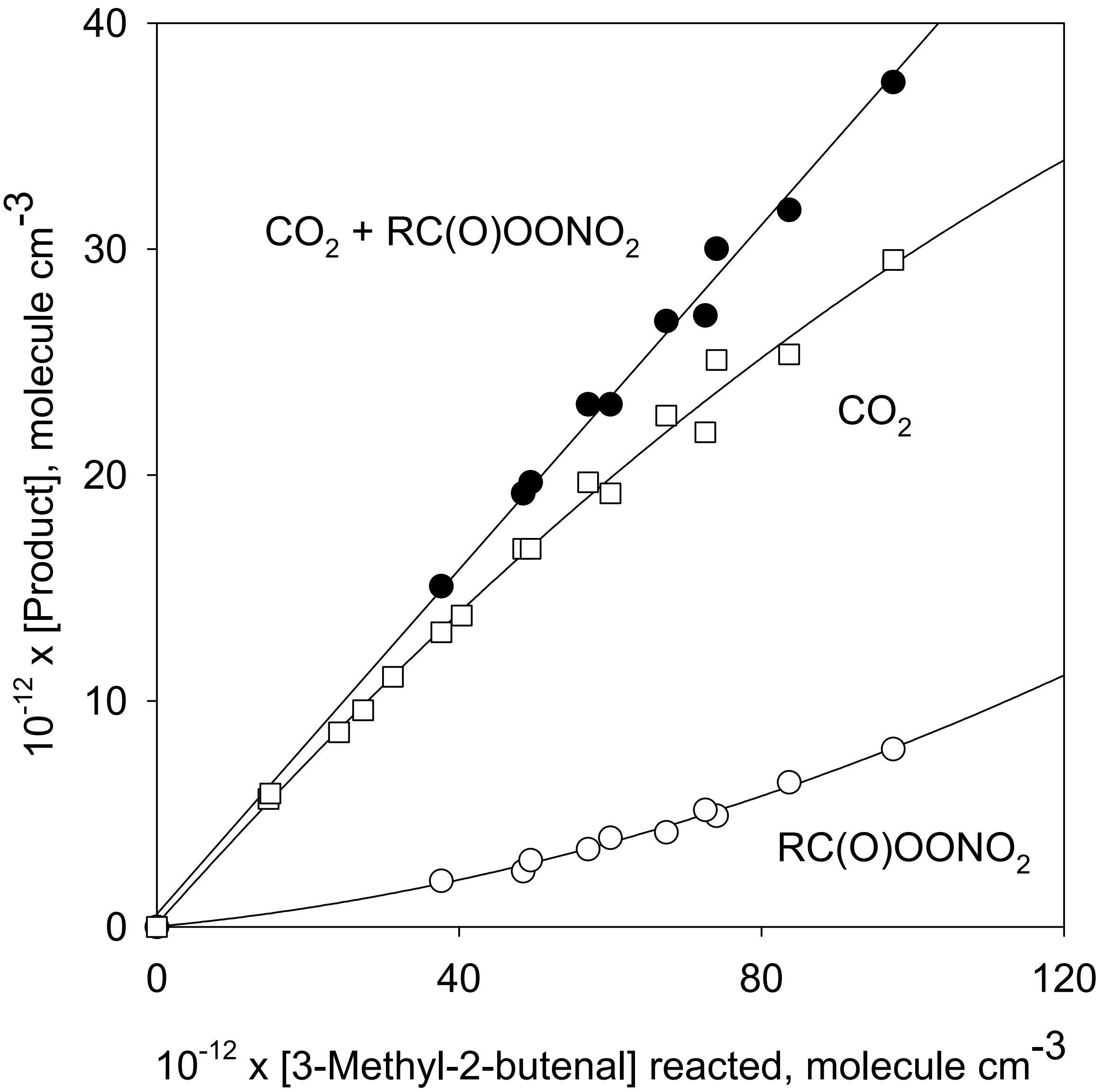

Figure 12. Plots of the amounts of CO_2, peroxyacyl nitrates ($RC(O)OONO_2$), and the sum of the amounts of CO_2 and $RC(O)OONO_2$ formed against the amounts of 3-methyl-2-butenal reacted with OH radicals. Analyses were by *in situ* FT-IR spectroscopy.

reactivity as 3-methyl-2-butenal towards the OH radical (as observed for CH_2=C(CH_3)C(O)OONO_2 (Orlando et al., 2002; IUPAC, 2006) and methacrolein (Atkinson and Arey, 2003; IUPAC, 2006), both of which have rate constants for reaction with OH radicals at 298 K of 2.9 x 10^{-11} cm^3 $molecule^{-1}$ s^{-1}), no corrections for secondary reactions were made to the measured concentrations plotted in Figure 12. This may result in a slight underestimation of the RC(O)OONO_2 yield.

CO_2 was measured both from its band at 2350 cm^{-1} and from its sharp absorption feature at 668 cm^{-1}, taking into account the observed non-linearity in its analysis. The yield of CO_2 was observed to slowly decrease with irradiation time (Figure 12), with a yield of 39% early in the reaction decreasing to a yield of 30% at the end of one irradiation experiment. As evident from Figure 12, a plot of the sum of the CO_2 and RC(O)OONO_2 concentrations against the amount of 3-methyl-2-butenal reacted resulted in a yield of (CO_2 + RC(O)OONO_2) which was independent of the extent of reaction, with a combined yield of 38 ± 6% (Table 5). As noted above, the peroxyacyl nitrate formed in this reaction is expected to react with OH radicals, and since we have not corrected the measured RC(O)OONO_2 data for secondary reactions the sum of the CO_2 and RC(O)OONO_2 yields may be a slight underestimate. Assuming that the RC(O)OONO_2 formed in this reaction, attributed to $(CH_3)_2$C=CHC(O)OONO_2 (see below), is comparable in reactivity towards the OH radical as is 3-methyl-2-butenal, then applying the correction for secondary reaction with OH radicals assuming that RC(O)OONO_2 is formed with a constant yield from 3-methyl-2-butenal increases the yield of (CO_2 + RC(O)OONO_2) to 43 ± 7%. In reality, the formation yield of RC(O)OONO_2 increases with the extent of reaction (Figure 12) and hence this procedure overcorrects for secondary reaction with OH radicals.

Product Analyses by SPME/GC-FID and SPME/GC-MS. GC-MS analyses of pre-coated SPME fibers exposed to irradiated CH_3ONO – NO - 3-methyl-2-butenal – air mixtures showed the presence of acetone, glyoxal and 2-hydroxy-2-methylpropanal, as the mono-oxime (acetone and 2-hydroxy-2-methylpropanal) and di-oxime (glyoxal) derivatives. 2-Hydroxy-2-methylpropanal was identified by matching the GC retention time and MS spectrum of its oxime with that of the same product formed in the OH radical-initiated reaction of 2-methyl-3-buten-2-ol (Reisen et al., 2003b). Three sets of sequential CH_3ONO – NO – 3-methyl-2-butenal – air and CH_3ONO – NO – 2-methyl-3-buten-2-ol – air irradiations were carried out, with similar initial concentrations and experimental conditions for each set of sequential experiments and with Tenax/GC-FID analysis of 3-methyl-2-butenal and 2-methyl-3-buten-2-ol and SPME/GC-FID analysis of 2-hydroxy-2-methylpropanal. The measured amounts of 2-hydroxy-2-methylpropanal were corrected for secondary reactions with the OH radical using rate constants (in units of 10^{-11} cm^3 $molecule^{-1}$ s^{-1}) of: 3-methyl-2-butenal, 6.21 (this work); 2-methyl-3-buten-2-ol, 6.4 (IUPAC, 2006); and 2-hydroxy-2-methylpropanal, 1.5 (IUPAC, 2006), with the corrections being 8-12%. Using Equation (III) and a yield of 2-hydroxy-2-methylpropanal from the OH radical-initiated reaction of 2-methyl-3-buten-2-ol of 31% (Reisen et al., 2003b), the three sets of experiments lead to formation yields of 2-hydroxy-2-methylpropanal from 3-methyl-2-butenal of 4.6%, 4.5% and 4.6%. The average yield is given in Table 6.

2-1.3. Discussion

The rate constant measured here for the reaction of OH radicals with 3-methyl-2-butenal is the first reported. The room temperature rate constants for acrolein, crotonaldehyde, methacrolein and 3-methyl-2-butenal increase with the number of methyl-substituents around the

C=C bond, and are (in units of 10^{-11} cm^3 $molecule^{-1}$ s^{-1}): acrolein [CH_2=CHCHO], 2.0 (Atkinson, 1994; Magneron et al., 2002); crotonaldehyde [CH_3CH=CHCHO], 3.5 (Atkinson, 1994; Magneron et al., 2002); methacrolein [CH_2=C(CH_3)CHO], 2.9 (Arey and Atkinson, 2003; IPUAC, 2006); and 3-methyl-2-butenal [$(CH_3)_2C$=CHCHO], 6.2 (this work). This increase in rate constant with the number of methyl substituents is consistent with OH radical addition to the C=C bond being important. A similar effect of methyl substitution on the rate constants is observed for reaction of OH radicals with ethene and the methyl-substituted alkenes (Arey and Atkinson, 2003). The estimation method of Kwok and Atkinson (1995) leads to a calculated rate constant at 298 K of 4.7 x 10^{-11} cm^3 $molecule^{-1}$ s^{-1}, 25% lower than our measured value, with H-atom abstraction from the CHO group being estimated to account for 36% of the overall reaction and OH radical addition at the C=C bond for the remainder (Kwok and Atkinson, 1995).

By analogy with other α,β-unsaturated aldehydes, the reaction of OH radicals with 3-methyl-2-butenal proceeds by H-atom abstraction from the C-H bond of the CHO group and by addition to the carbon atoms of the C=C bond (Tuazon and Atkinson, 1990; Kwok and Atkinson, 1995; Magneron et al., 2002; Orlando and Tyndall, 2002).

$$OH + (CH_3)_2C{=}CHCHO \rightarrow H_2O + (CH_3)_2C{=}CHC^{\bullet}O \qquad (1a)$$

$$OH + (CH_3)_2C{=}CHCHO \rightarrow (CH_3)_2C^{\bullet}CH(OH)CHO \qquad (1b)$$

$$OH + (CH_3)_2C{=}CHCHO \rightarrow (CH_3)_2C(OH)C^{\bullet}HCHO \qquad (1c)$$

The acyl radical $(CH_3)_2C{=}CHC^{\bullet}O$ formed in reaction (1a) is expected to rapidly add O_2 [reaction (3)], and then react with NO_2 [reaction (4)] to form a peroxyacyl nitrate, or with NO [reaction (5)].

$$(CH_3)_2C{=}CHC^{\bullet}O + O_2 + M \rightarrow (CH_3)_2C{=}CHC(O)OO^{\bullet} + M \qquad (3)$$

$$(CH_3)_2C{=}CHC(O)OO^{\bullet} + NO_2 + M \leftrightarrow (CH_3)_2C{=}CHC(O)OONO_2 + M \qquad (4)$$

$$(CH_3)_2C{=}CHC(O)OO^{\bullet} + NO \rightarrow (CH_3)_2C{=}CHC(O)O^{\bullet} + NO_2 \qquad (5)$$

The $(CH_3)_2C{=}CHC(O)O^{\bullet}$ radical is expected to rapidly decompose,

$$(CH_3)_2C{=}CHC(O)O^{\bullet} \rightarrow (CH_3)_2C{=}C^{\bullet}H + CO_2 \qquad (6)$$

with the 1,1-dimethylvinyl radical possibly reacting with O_2 to form acetone plus, ultimately, CO (Atkinson, 1989).

$$(CH_3)_2C{=}C^{\bullet}H + O_2 \rightarrow CH_3C(O)CH_3 + HC^{\bullet}O \qquad (7)$$

$$HC^{\bullet}O + O_2 \rightarrow CO + HO_2 \qquad (8)$$

The $(CH_3)_2C^{\bullet}CH(OH)CHO$ and $(CH_3)_2C(OH)C^{\bullet}HCHO$ radicals formed after OH radical addition (reactions (1b) and (1c), respectively) will rapidly add O_2 to form the corresponding 1,2-hydroxyperoxy radicals and then, under our experimental conditions, react with NO to form either a 1,2-hydroxynitrate or a 1,2-hydroxyalkoxy radical plus NO_2 (Atkinson and Arey, 2003),

$$(CH_3)_2C^{\bullet}CH(OH)CHO + O_2 \rightarrow (CH_3)_2C(OO^{\bullet})CH(OH)CHO \quad (9)$$

$$(CH_3)_2C(OO^{\bullet})CH(OH)CHO + NO \rightarrow (CH_3)_2C(ONO_2)CH(OH)CHO \quad (10)$$

$$(CH_3)_2C(OO^{\bullet})CH(OH)CHO + NO \rightarrow (CH_3)_2C(O^{\bullet})CH(OH)CHO + NO_2 \quad (11)$$

and analogously for the $(CH_3)_2C(OH)C^{\bullet}HCHO$ radical, forming $(CH_3)_2C(OH)CH(ONO_2)CHO$ or $(CH_3)_2C(OH)CH(O^{\bullet})CHO$ plus NO_2.

The 1,2-hydroxyalkoxy radicals are expected to dominantly decompose, because isomerization through a 6-membered transition state cannot occur and decomposition is expected to dominate over reaction with O_2 (Tuazon and Atkinson, 1990; Magneron et al., 2002; Orlando and Tyndall, 2002).

$$(CH_3)_2C(O^{\bullet})CH(OH)CHO \rightarrow CH_3C(O)CH_3 + HOC^{\bullet}HCHO \quad (12)$$

$$HOC^{\bullet}HCHO + O_2 \rightarrow (CHO)_2 + HO_2 \quad (13)$$

$$(CH_3)_2C(OH)CH(O^{\bullet})CHO \rightarrow (CH_3)_2C(OH)CHO + HC^{\bullet}O \quad (14)$$

$$(CH_3)_2C(OH)CH(O^{\bullet})CHO \rightarrow CH_3C^{\bullet}(OH)CH_3 + (CHO)_2 \quad (15)$$

$$CH_3C^{\bullet}(OH)CH_3 + O_2 \rightarrow CH_3C(O)CH_3 + HO_2 \quad (16)$$

Therefore, the products from the OH radical addition pathway are expected to be the 1,2-hydroxynitrates $(CH_3)_2C(ONO_2)CH(OH)CHO$ and $(CH_3)_2C(OH)CH(ONO_2)CHO$, acetone + glyoxal, and 2-hydroxy-2-methylpropanal + CO, and the products from the H-atom abstraction pathway are expected to be the peroxyacyl nitrate $(CH_3)_2C{=}CHC(O)OONO_2$ or acetone + CO + CO_2 (and possibly other products of the atmospheric reactions of the $(CH_3)_2C{=}C^{\bullet}H$ radical). Based on the kinetic and product data for methacrolein (Tuazon and Atkinson, 1990; Orlando et al., 1999; Atkinson and Arey, 2003; IUPAC, 2006) and $CH_2{=}C(CH_3)C(O)OONO_2$ (Orlando et al., 2002; IUPAC, 2006), OH radicals are expected to react with $(CH_3)_2C{=}CHC(O)OONO_2$ with a rate constant comparable to that for the reaction of OH radicals with 3-methyl-2-butenal to form, at least in part, acetone.

These predictions are totally consistent with the products identified and quantified here. Thus the organic nitrates observed, with a molar yield of $8.5 \pm 2.3\%$, are attributed to the hydroxynitrates $(CH_3)_2C(ONO_2)CH(OH)CHO$ and $(CH_3)_2C(OH)CH(ONO_2)CHO$. Our measured glyoxal and 2-hydroxy-2-methylpropanal yields of $40 \pm 3\%$ and $4.6 \pm 0.7\%$, combined with the organic nitrate yield, therefore show that the OH radical addition pathway accounts for $53 \pm 4\%$ of the overall reaction.

Acetone is formed from one channel of the OH radical addition pathway (as a co-product to glyoxal) and is an expected product of the $(CH_3)_2C{=}C^{\bullet}H + O_2$ reaction [reaction (7)]. The fraction of the acyl peroxy radicals, $(CH_3)_2C{=}CHC(O)OO^{\bullet}$, formed in the H-atom abstraction pathway which form the peroxyacyl nitrate $(CH_3)_2C=CHC(O)OONO_2$ depends on the NO_2/NO concentration ratio and is thus expected to increase with the extent of reaction (with NO being converted to NO_2 as the reaction proceeds by reactions of NO with HO_2 and organic peroxy radicals), and this is observed (Figure 12). This increase in formation yield of $(CH_3)_2C=CHC(O)OONO_2$ with extent of reaction is compensated by a corresponding decrease in CO_2 yield [reaction (4) being competitive with reaction (5) followed by reaction (6)] and with the sum of the yields of CO_2 and $(CH_3)_2C=CHC(O)OONO_2$ being the fraction of the overall reaction proceeding by H-atom abstraction from the CHO group. We attribute the peroxyacyl nitrate observed to $(CH_3)_2C=CHC(O)OONO_2$. The sum of the CO_2 and $RC(O)OONO_2$ yields, and hence the percentage of the overall reaction proceeding by H-atom abstraction from the CHO group, is 38 ± 6% neglecting any losses of $(CH_3)_2C=CHC(O)OONO_2$ due to reaction with OH radicals.

The acetone yield, based on our measured yields of its co-products CO_2 (from the H-atom abstraction channel) and glyoxal (from the OH radical addition channel) is expected to be initially 79%, decreasing with extent of reaction to ~70% at the end of the reactions, if the $(CH_3)_2C=C^{\bullet}H$ radical reacts with O_2 [reaction (7)] to form acetone in unit yield. Our measured acetone yield of 74 ± 6% is in good agreement with that expected, and a least-squares analysis showed that the acetone formed is 105 ± 3% of the sum of the glyoxal (corrected for secondary reactions) and CO_2 formed, where the indicated error is two least-squares standard deviations. This agreement indicates that the $(CH_3)_2C=C^{\bullet}H$ radical reacts with O_2 to form acetone in unit yield [reaction (7)], and also suggests that secondary reactions of $(CH_3)_2C=CHC(O)OONO_2$ with OH radicals to form acetone were relatively minor under our experimental conditions.

As noted above, an additional small potential source of acetone is from the reaction of $(CH_3)_2C=CHC(O)OONO_2$ with OH radicals. Hence the sum of the yields of acetone and $RC(O)OONO_2$ should represent the fraction of the overall OH radical reaction with 3-methyl-2-butenal proceeding by H-atom abstraction from the CHO group plus the portion of the OH addition channel leading to formation of glyoxal plus acetone. Least-squares analysis results in a sum of the yields of acetone and $RC(O)OONO_2$ of 82 ± 8% (Table 6). Subtracting the acetone formed as a co-product to glyoxal (40 ± 3%) results in the H-atom abstraction pathway accounting for 42 ± 9% of the overall OH radical reaction, consistent with the value of 38 ± 6% obtained from the sum of the CO_2 and $RC(O)OONO_2$ yields and neglecting any reactive losses of $RC(O)OONO_2$.

Our product yield data account for 91 ± 8% (from the sum of the glyoxal, 2-hydroxy-2-methylpropanal, $RONO_2$ and CO_2 + $RC(O)OONO_2$ yields) or 95 ± 9% (from the sum of the 2-hydroxy-2-methylpropanal, $RONO_2$ and acetone + $RC(O)OONO_2$ yields) of the reaction pathways. Interestingly, the fraction of the overall reaction proceeding by H-atom abstraction from the CHO group in 3-methyl-2-butenal (~40%) is only slightly less than the measured fraction of the overall reaction with methacrolein proceeding by H-atom abstraction [50% (Tuazon and Atkinson, 1990) and 45% (Orlando et al., 1999)], despite the factor of 2 higher rate constant for the OH radical reaction with 3-methyl-2-butenal compared to that with methacrolein. Decomposition of the $(CH_3)_2C(OH)CH(O^{\bullet})CHO$ radical via reaction (14) is thermochemically favored over decomposition via reaction (15). If the $(CH_3)_2C(OH)CH(O^{\bullet})CHO$ radical decomposes preferentially via reaction (14) to form 2-hydroxy-2-methylpropanal, then the OH radical appears to add preferentially to the carbonyl-substituted carbon atom in the C=C bond [reaction (1b)] compared to addition to the other carbon atom [reaction (1c)], by an ~10:1 ratio, analogous to the methacrolein reaction (Tuazon and Atkinson, 1990).

2-1.4. Conclusions

The relatively high yield of glyoxal of 40 ± 3% and the high reactivity of 3-methyl-2-butenal towards the OH radical (therefore minimizing secondary reactions of glyoxal with OH radicals) makes this reaction a good *in situ* source of glyoxal for calibration of our SPME on-fiber derivatization method (see B 2-2. below).

2-2. Measurement of the Glyoxal Formation Yield from OH + Naphthalene as a Function of NO_x Concentration

Glyoxal has been observed as a product of the gas-phase reaction of OH radicals with naphthalene (Reisen, 2003). We have previously measured the formation yields of 2,3-butanedione [$CH_3C(O)C(O)CH_3$] and 3-hexene-2,5-dione [$CH_3C(O)CH=CHC(O)CH_3$] from the OH radical-initiated reactions of *o*- and *p*-xylene and 1,2,3- and 1,2,4-trimethylbenzene (Atkinson and Aschmann, 1994; Bethel et al., 2000]. In all cases, the formation yields of these dicarbonyls decreased with increasing NO_2 concentration over the range 0.2-5.3 ppmv, indicating that the OH-aromatic adducts were reacting with O_2 and NO_2 and that these competing OH-aromatic adduct reactions have different dicarbonyl formation yields. Assuming that the glyoxal formation yields from the OH-naphthalene adducts with O_2 and NO_2 differ significantly and that the NO_2 reaction dominates at NO_2 concentrations >1 ppmv [consistent with the limited literature nitronaphthalene yield data (Atkinson et al., 1987)], then measurement of the glyoxal formation yield from the reaction of OH radicals with naphthalene as a function of the NO_2 (or NO_x) concentration should indicate the NO_2 concentration regime where the O_2 and NO_2 reactions with the OH-naphthalene adducts are competitive. We therefore measured the formation yield of glyoxal from this reaction using SPME fibers pre-coated with PFBHA for derivatization of glyoxal, with subsequent analysis by GC-FID.

2-2.1. Experimental Methods

Experiments were carried out in a 7000 liter Teflon chamber, with two parallel banks of blacklamps for irradiation. Hydroxyl radicals were produced in the presence of NO_x by the photolysis of methyl nitrite (CH_3ONO) in air at wavelengths >300 nm, with NO being included in the initial reactants to suppress the formation of O_3 and of NO_3 radicals (see (A) above). In addition, OH radicals were generated in the absence of added NO_x from the dark reaction of O_3 with alkenes (Atkinson and Aschmann, 1993; Chew and Atkinson, 1996). The alkene(s) used had to be reasonably reactive towards O_3 (with reaction rate constants >5 x 10^{-17} cm^3 $molecule^{-1}$ s^{-1}) and be known or expected to lead to significant OH radical production. Several alkenes were investigated to determine whether they formed glyoxal from their reaction with O_3, by carrying out experiments in the absence of naphthalene. While glyoxal was not observed from the 2-methyl-2-butene reaction, methylglyoxal was observed as a product and the GC peaks of the oximes of methylglyoxal overlapped with two of the GC peaks due to the oximes of glyoxal. The other alkenes investigated (*trans*-2-butene, *trans*-3-hexene, cyclohexene and α-pinene) resulted in the formation of glyoxal, and hence could not be used as the OH radical precursor for measuring glyoxal formation from the reaction of OH radicals with naphthalene. 2-Methyl-2-butene was therefore used to generate OH radicals in the absence of NO_x.

Solid Phase MicroExtraction (SPME) fibers were pre-coated with PFBHA [*O*-(2,3,4,5,6-pentafluorobenzyl)hydroxylamine] to allow on-fiber derivatization of glyoxal, with subsequent thermal desorption and gas chromatographic analysis of glyoxal as its di-derivatized oximes. Note that no significant GC peaks arising from the mono-oximes were observed. The SPME/GC-FID analysis method was periodically calibrated by generating known concentrations of glyoxal *in situ* in the chamber from the reaction of OH radicals with 3-methyl-2-butenal, which forms glyoxal in 40 ± 3% yield as described above in (B) 2-1. The initial naphthalene concentrations were in the range (0.37-3.01) x 10^{13} molecule cm^{-3}. When OH radicals were generated by the photolysis of methyl nitrite in air, the initial CH_3ONO and NO concentrations were varied in the range (0.24-12) x 10^{13} molecule cm^{-3}, with the initial [CH_3ONO] = [NO]. When OH radicals were generated from the dark reaction of O_3 with 2-methyl-2-butene, the initial 2-methyl-2-butene concentration was ~2.4 x 10^{13} molecule cm^{-3}, and 3 additions of 50 cm^3 of O_3 in O_2 diluent were added during an experiment. The O_3 in O_2 diluent was generated as needed by a Welsbach T-408 ozone generator.

2-2.2 Results and Discussion

A series of experiments were carried out in which OH radicals (generated from photolysis of methyl nitrite or from the dark reaction of O_3 with 2-methyl-2-butene) were reacted with naphthalene in the presence of varying amounts of NO_x. In all experiments, the measured glyoxal concentrations were corrected for secondary reaction with OH radicals, with the correction increasing with the extent of reaction of naphthalene (Atkinson et al., 1982) and typically being <10%. In one experiment carried out to 60% reactive consumption of the initial naphthalene (the data denoted by ∇ in Figure 13), within the experimental errors the glyoxal yield was independent of the extent of reaction. This indicated that glyoxal was not formed to any significant extent as a second-generation product and that the measured glyoxal formation yields refer to formation as a first-generation product from naphthalene. A possible pathway to formation of glyoxal as a second-generation product is from the reaction of OH radicals with 2-formylcinnamaldehyde, leading to glyoxal + phthaldialdehyde (Sasaki et al., 1997), as shown in Scheme 3 for OH radical addition at one of the two carbons of the C=C bond (OH radical addition at the other carbon of the C=C bond leads to the same products by an analogous set of reactions)]. The observation that secondary formation of glyoxal is of minor or negligible importance suggests that phthaldialdehyde is also formed as a first-generation product with little or no second-generation formation. This is consistent with data obtained for formation of phthaldialdehyde from the OH radical-initiated reaction of naphthalene using API-MS for analysis as a function of the extent of reaction of naphthalene (unpublished data from CARB Contract 03-314).

Representative plots of the amounts of glyoxal formed, corrected for secondary reaction with OH radicals, against that amounts of naphthalene reacted with OH radicals are shown in Figure 13. At the lower initial CH_3ONO and NO concentrations, the initial naphthalene concentration was also decreased to slow down the rate of NO-to-NO_2 conversion (and hence the onset of O_3 and NO_3 radical formation), and this resulted in only small amounts of naphthalene reacted, as evident from Figure 13. The resulting glyoxal formation yields, obtained from the slopes of the plots in Figure 13 by least-squares analyses, are plotted against the initial NO concentration in Figure 14. The indicated error bars are the least-squares two-standard deviation,

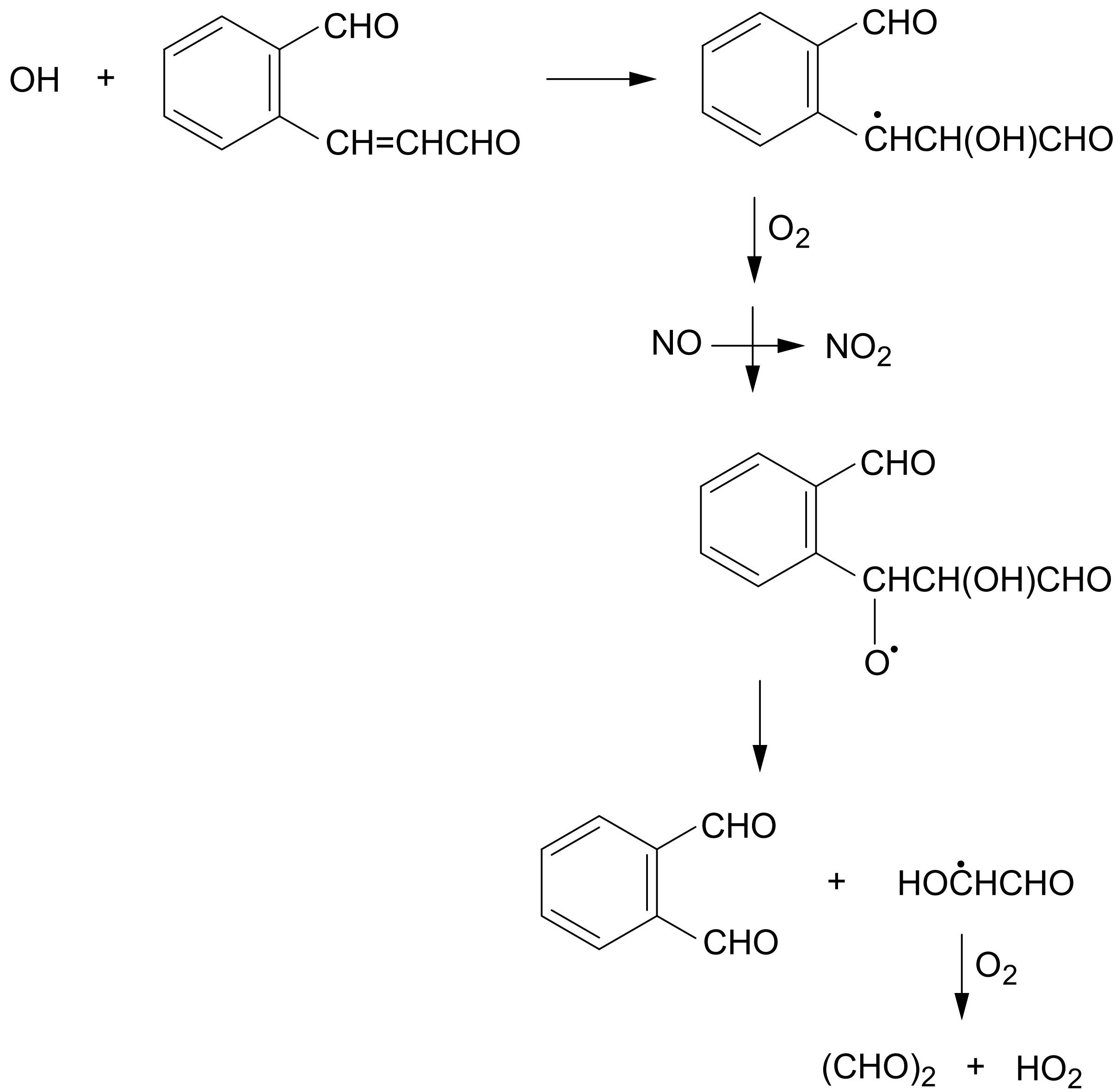

Scheme 3

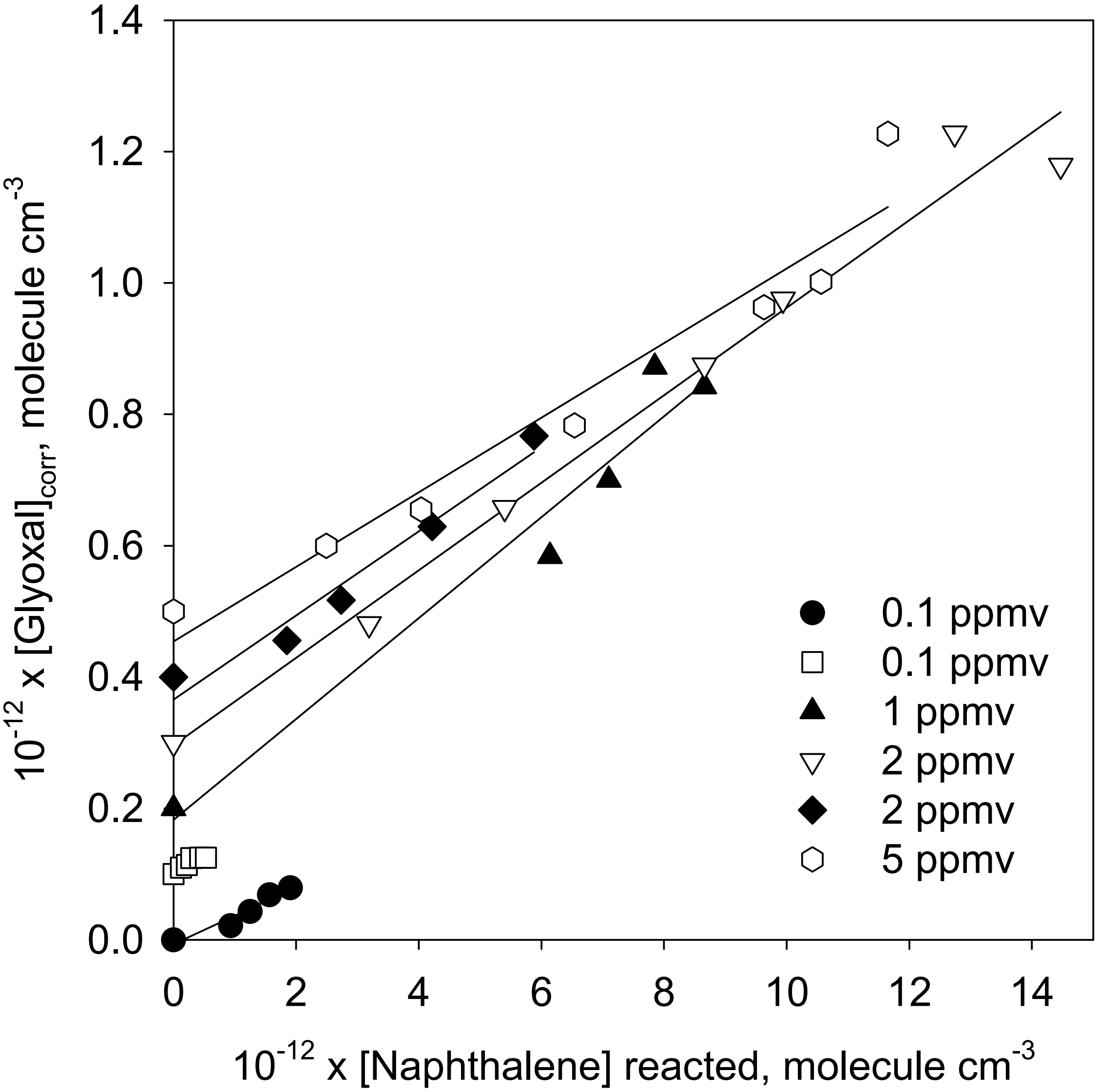

Figure 13. Representative plots of the amounts of glyoxal formed, corrected for reaction with OH radicals (see text) against the amounts of naphthalene reacted in irradiated CH_3ONO – NO – naphthalene – air mixtures at various initial NO concentrations (in each case, the initial CH_3ONO and NO concentrations were equal). The glyoxal data are offset vertically by varying amounts for clarity.

and the uncertainties tend to increase as the initial CH_3ONO (the photolytic precursor to OH radicals) and NO concentrations decrease because of a decreasing fraction of the initially present naphthalene being consumed by reaction. Within the often rather large experimental uncertainties, there is no obvious dependence of the glyoxal formation yield on the initial NO_x concentration. Using the simple average of all of the data in Figure 14 (the solid horizontal line), the glyoxal yield from the OH + naphthalene reaction is 6 ± 2% over the NO_x range ≤0.1 to 5 ppmv.

This independence of the glyoxal formation yield with initial NO_x suggests that the mechanism leading to glyoxal formation from naphthalene does not change as the NO_x concentration is varied. Since it appears from the relative invariance of the 1- and 2-nitronaphthalene formation yields from the OH radical-initiated reaction of naphthalene observed by Atkinson et al. (1987) at NO_2 concentrations of 2-7 ppmv that at ppmv levels of NO_2 the initially formed OH-naphthalene adduct reacts with NO_2, this then suggests that the OH-naphthalene adduct reacts with NO_2 down to NO_2 levels <0.1 ppm (because $[NO_2] \leq [NO_x]$). However, it is possible that the glyoxal formation yields from the reactions of the OH-naphthalene adducts with O_2 and NO_2 are similar, in which case we would not see any effect of NO_x concentration on the glyoxal yield. A more definitive probe of one of the OH-naophthalene adduct reactions is clearly preferable, and our preliminary work on such a direct observation of the OH-naphthalene adduct + NO_2 reaction is presented in Section B 2-3 below.

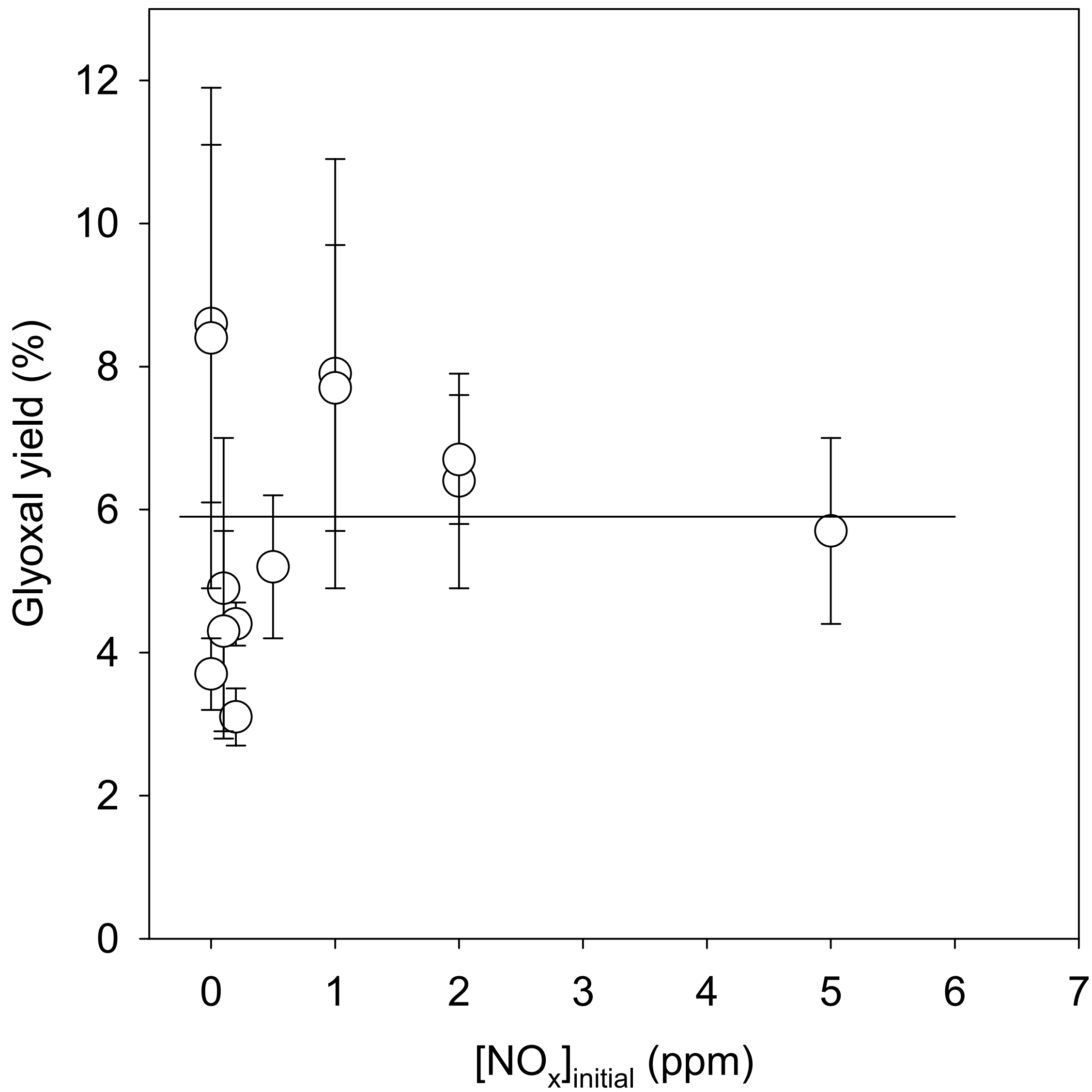

Figure 14. Plot of glyoxal formation yield from the reaction of OH radicals with naphthalene as a function of the initial NO_x concentration.

2-3. Formation Yields of Nitronaphthalenes and other Nitro-Aromatics from the OH Radical-Initiated Reactions of Aromatic Hydrocarbons and PAHs as a Function of NO_x Concentration

As discussed above, the reactions leading to nitroaromatic production from the OH radical-initiated reactions of aromatic hydrocarbons (including PAHs) are believed to involve:

OH + aromatic → OH-aromatic adduct (k_a)

OH-aromatic adduct + O_2 → products (k_{O2})

OH-aromatic adduct + NO_2 → α nitroaromatic (+ other products) (k_{NO2})

where k_{O2} and k_{NO2} are the rate constants for the reactions of the OH-aromatic adduct(s) with O_2 and NO_2, respectively, and α is the nitroaromatic yield from the NO_2 + OH-aromatic adduct reaction. Therefore, the nitroaromatic formation yield is given by:

$$\text{nitroaromatic formation yield} = \alpha k_{NO2}[NO_2]/(k_{O2}[O_2] + k_{NO2}[NO_2]) \qquad \text{IV}$$

and at NO_2 concentrations such that $k_{O2}[O_2] > k_{NO2}[NO_2]$ the nitro-aromatic yield decreases with decreasing NO_2 concentration. For the aromatic hydrocarbons benzene, toluene and the xylenes, the NO_2 concentrations at which $k_{NO2}[NO_2] = k_{O2}[O_2]$ are in the range ~1-5 ppmv and under atmospheric conditions (even in heavily polluted urban areas) the reactions of the OH-aromatic hydrocarbons with O_2 dominate and nitroaromatic formation is essentially negligible. Furthermore, the formation yields of 1,2-dicarbonyls and unsaturated 1,4-dicarbonyls decrease with increasing NO_2, consistent with the change-over in mechanism from reaction of the OH-aromatic with O_2 to being with NO_2 (Atkinson and Aschmann, 1994; Bethel et al., 2000). However, no analogous laboratory data exist for the OH + PAH reactions, and as a complementary, and potentially more direct, approach to our measurements of the glyoxal yield as a function of NO_x (Section B 2-2. above), we conducted preliminary experiments to investigate the formation yields of selected nitro-aromatic products from the OH radical-initiated reactions of the parent aromatic hydrocarbon as a function of NO_x concentration. The aromatic hydrocarbons chosen were toluene, naphthalene and biphenyl, with the nitro-products being 3-nitrotoluene, 1- and 2-nitronaphthalene and 3-nitrobiphenyl, respectively (Atkinson et al., 1987, 1989; Sasaki et al., 1997). These were chosen because of prior studies carried out in this laboratory (Atkinson et al., 1987, 1989; Atkinson and Aschmann, 1994; Sasaki et al., 1997) and the relatively extensive knowledge of the reactions of the OH-toluene adducts (Knispel et al., 1990; Bohn, 2001). Toluene and biphenyl have similar reactivities towards OH radicals and do not react at measurable rates with NO_3 radicals, while naphthalene is a factor of 3-4 more reactive towards reaction with OH radicals and also reacts with NO_3 radicals (Atkinson and Arey, 2003; Table 1).

2-3.1. Experimental Methods

A major effort was made to develop the optimum analytical protocols to measure the aromatic hydrocarbons and their nitro-products during the experiments, recognizing that the nitro-aromatic yields are in the range ~0.5-10% at high (ppmv) NO_2 concentrations (Atkinson et al., 1987; Atkinson and Aschmann, 1994; Sasaki et al., 1997) but can be orders of magnitude lower, at least for 3-nitrotoluene, at lower NO_2 concentrations (Atkinson and Aschmann, 1994). After much trial and error, it was determined that the following analysis methods appear to work:

- Collection of gas samples onto Tenax-TA solid adsorbent with subsequent thermal desorption onto a DB-5 megabore column for GC-FID analysis of toluene and naphthalene.
- Exposure of a 100 μm PDMS (polydimethylsiloxane) fiber to the chamber contents with subsequent thermal desorption onto a DB-5 megabore column for GC-FID analysis of naphthalene and biphenyl.
- Exposure of a 65μm PDMS/DVB (polydimethylsiloxane/divinylbenzene) fiber to the chamber contents with subsequent thermal desorption onto a DB-17 capillary column for combined gas chromatography-negative ion chemical ionization mass spectrometry (GC-NICIMS) analysis of 3-nitrotoluene, 1- and 2-nitronaphthalene and 3-nitrobiphenyl.

A known amount of nitrobenzene was introduced into the chamber in all chamber experiments to serve as an internal standard for the GC-NICIMS analyses of the nitro-aromatics, and the GC-NICIMS instrument was calibrated for the nitro-aromatics by introducing known amounts of 3-nitrotoluene, 1-nitronaphthalene, 2-nitronaphthalene and 3-nitrobiphenyl into the chamber, these ranging from 0.03-8.5 ppbv in each case. The SPME-sampling/GC-NICIMS response factors were found to depend on the nitroaromatic concentration in each case, and calibration curves were constructed for each nitro-product.

Experiments have been carried out in a 7000 liter Teflon chamber, with OH radicals generated by the photolysis of CH_3ONO – NO – air mixtures (initial NO_x mixing ratios of 0.1-10 ppmv) and from the reaction of O_3 with 2-methyl-2-butene with 0.02-0.2 ppmv of NO_2 initially present. In the latter system, the reactions are

$O_3 + (CH_3)_2C{=}CHCH_3 \rightarrow \alpha\ OH$ + other products

$O_3 + NO_2 \rightarrow NO_3 + O_2$

$OH + (CH_3)_2C{=}CHCH_3 \rightarrow$ products

OH + aromatic $\rightarrow$ products (including nitro-aromatics)

$NO_3 + (CH_3)_2C{=}CHCH_3 \rightarrow$ products

NO_3 + naphthalene $\rightarrow$ products (including nitronaphthalenes)

Based on the literature rate constants for the reactions of O_3 with 2-methyl-2-butene [4.0×10^{-16} cm^3 $molecule^{-1}$ s^{-1} (Atkinson and Arey, 2003)] and NO_2 [3.5×10^{-17} cm^3 $molecule^{-1}$ s^{-1} (IUPAC, 2006)], at the maximum NO_2 concentrations used ≤4% of the O_3 would react with NO_2 to form NO_3 radicals. These NO_3 radicals would react dominantly (>99.9%) with 2-methyl-2-butene and it is calculated that nitronaphthalene formation from the NO_3 radical-initiated reaction of naphthalene should be of no importance (note that toluene and biphenyl do not react at measurable rates with NO_3 radicals [Table 1]). Because NO_3 radical formation could be important in the photolysis of CH_3ONO – NO – air mixtures at low initial CH_3ONO and NO concentrations (due to NO-to-NO_2 conversion by HO_2 and organic peroxy radicals), we added 2-methyl-2-butene immediately after the single irradiation period to attempt to scavenge any NO_3 radicals present.

The initial toluene, naphthalene and biphenyl concentrations (molecule cm^{-3} units) were ~2.4 x 10^{13} (1 ppmv), ~4.8 x 10^{13} (2 ppmv) and ~2.4 x 10^{13} (1 ppmv), respectively. When added for OH radical generation from the O_3 reaction, the initial 2-methyl-2-butene concentration was ~2.4 x 10^{13} molecule cm^{-3} (1 ppmv). For OH radical generation from the photolysis of methyl nitrite, the initial CH_3ONO and NO concentrations were equal, and ranged from (0.48-24) x 10^{13} molecule cm^{-3} each.

2-3.2. Results and Discussion

The data obtained during this contract were an investigation of the effect of NO_x concentration on the 3-nitrotoluene yield from toluene and the development of methods (see above) to allow similar data to be obtained for nitronaphthalenes from napththalene and 3-nitrobiphenyl from biphenyl. A series of experiments using the two OH radical generation methods were carried, and the data obtained for the formation of 3-nitrotoluene from toluene are plotted in Figure 15. While the data presented in Figure 15 are not absolute (*i.e.*, they are based on area counts for the various GC-FID or GC-NICIMS peaks, with allowance for the SPME-sampling/GC-NICIMS response of 3-nitrotoluene as a function of the amount of 3-nitrotoluene sampled being made) and hence the ratios (nitroaromatic formed/aromatic reacted) are in arbitrary units, what we are interested in is the behavior of the ratio (nitroaromatic formed/aromatic reacted) as a function of NO_x concentration. As evident from Figure 15, we have carried out experiments over the range 0.02-10 ppmv of initial NO_x [although the data point at the lowest NO_x concentration is subject to large uncertainties because the observed 3-nitrotoluene peak in the GC-NICIMS was lower in area than employed in the GC-NICIMS response factor calibration for 3-nitrotoluene (see caption to Figure 15)]. Nevertheless, the 3-nitrotoluene formation yield clearly decreases with decreasing NO_x concentration over the entire range of NO_x studied, and the behavior of the 3-nitroluene formation yield as a function of initial NO_x is very well fit by the solid line, which uses rate constants for the reactions of the OH-toluene adducts with O_2 and NO_2 of k_{O2} = 5.7 x 10^{-16} cm^3 $molecule^{-1}$ s^{-1} and k_{NO2} = 3.6 x 10^{-11} cm^3 $molecule^{-1}$ s^{-1} (Knispel et al., 1990; Bohn, 2001). The data shown in Figure 15 extend our previous, and much more limited, 3-nitrotoluene yield data (Atkinson and Aschmann, 1994) which ranged down to an NO_2 concentration of 0.65 ppmv. This excellent agreement between laboratory kinetic and mechanistic data and product yield data concerning the functional form of the 3-nitrotoluene formation yield dependence on NO_x concentration shows that we have a quantitative understanding of the reactions leading to atmospheric formation of 3-nitrotoluene from toluene.

We are now in the position of being able to carry out a much more extensive series of experiments, using the photolysis of methyl nitrite to generate OH radicals (as was done to obtain the experimental data in Figure 15) down to ~0.1 ppmv initial NO_x and the dark reaction of O_3 with 2-methyl-2-butene in the presence of NO_2 for the NO_2 concentration range ~0.02-0.1 ppmv. We therefore believe that in the future we could determine the formation yield of 1- and 2-nitronaphthalene and 3-nitrobiphenyl over a similar NO_x concentration range and determine the 1- and 2-nitronaphthalene and 3-nitrobiphenyl formation yields from their parent PAHs for realistic atmospheric conditions. The contract end date meant this could not be carried out during the present contract.

III. RECOMMENDATIONS FOR FUTURE RESEARCH

Based on the experimental studies carried out during this contract, the following studies are recommended:

- Measurement of the glyoxal and methylglyoxal formation yields from the gas-phase reactions of toluene, o-, m- and p-xylene and 1,2,3-, 1,2,4- and 1,3,5-trimethylbenzene as a function of the NO_2 concentration. To date, most measurements of the glyoxal and methylglyoxal formation yields from monocyclic aromatic hydrocarbons have been carried out at rather elevated NO_x concentrations and may not be applicable to ambient atmospheric conditions. This study would by analogous to those we have previously conducted for the formation of 2,3-butanedione and 3-hexene-2,5-dione (Atkinson and Aschmann, 1994; Bethel et al., 2000), and would provide a single extensive and systematic study of the effect of NO_2 concentration on the formation yields of these 1,2-dicarbonyls. Additionally, although absolute yield data would not be obtained, the effect of NO_2 concentration on the formation of the unsaturated 1,4-dicarbonyls observed in this contract [see section (A)] would be simultaneously determined.

- Investigate the formation yields of 1- and 2-nitronaphthalene and of 3-nitrobiphenyl from the OH radical-initiated reactions of naphthalene and biphenyl, respectively, as a function of NO_x concentration. This would provide the formation yield data needed to model the formation of these nitro-PAH under ambient atmospheric conditions and allow an assessment of the effect of reductions in NO_x emissions on atmospheric formation of nitro-PAHs from the OH radical-initiated reactions of gaseous PAHs. The laboratory nitro-aromatic yield data should be confirmed (or not) by analysis of ambient atmospheric daytime samples for 3-nitrotoluene, 1- and 2-nitronaphthalene, 3-nitrobiphenyl, toluene, naphthalene and biphenyl.

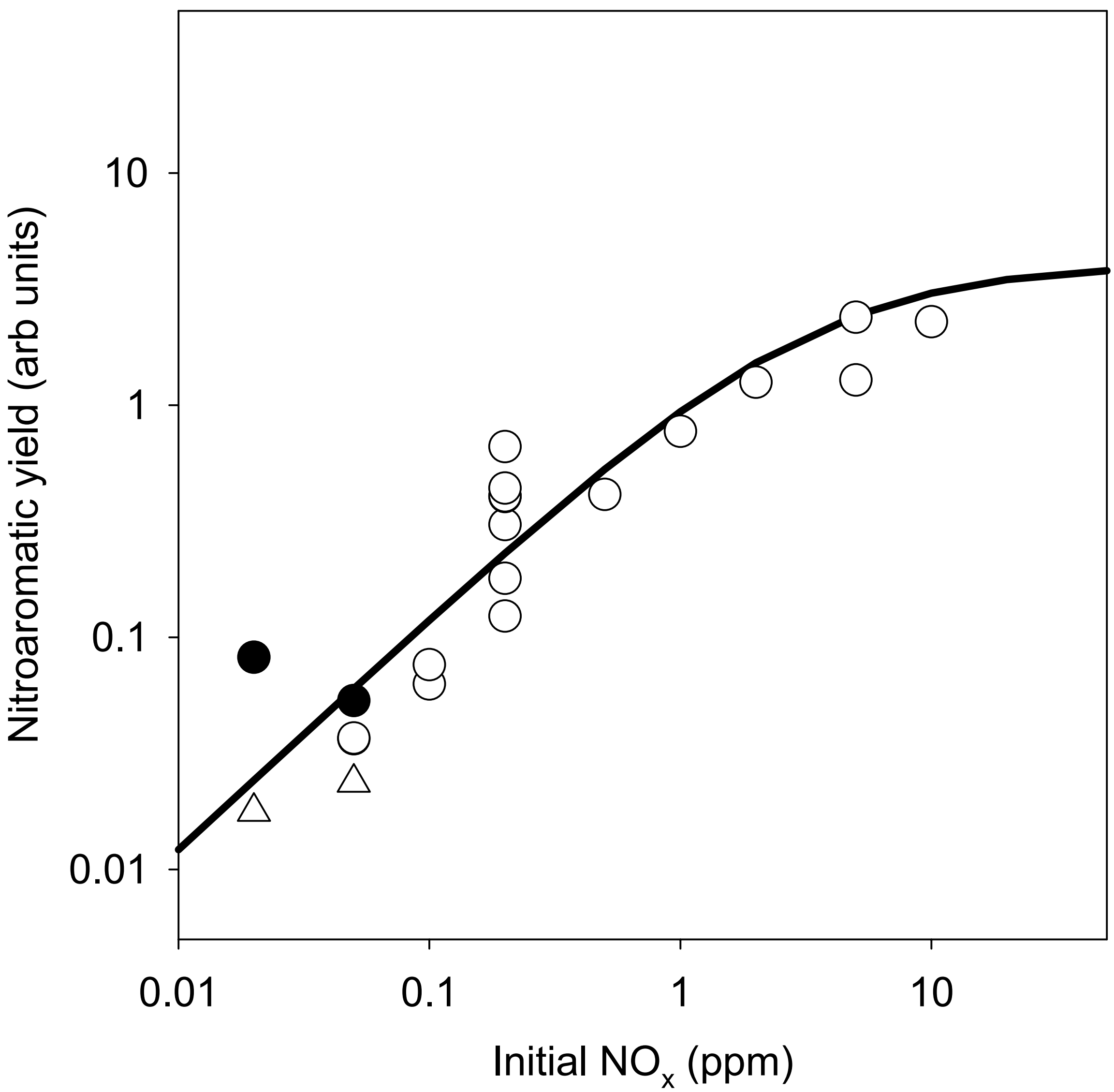

Figure 15. Plot of the 3-nitrotoluene formation yield (arbitrary units) against the initial NO_x concentration. ○ – 3-nitrotoluene concentrations calculated using the SPME sampling/GC-NICIMS calibration curve. For two of the three lowest NO_x experiments, the observed 3-nitrotoluene GC-NICIMS peak areas were below those used to generate the SPME sampling/GC-NICIMS calibration curve, and the 3-nitrotoluene yields are calculated using the calibration for the lowest 3-nitrotoluene concentration used to generate the calibration curve (Δ) or by an extrapolation of the calibration curve (•) The line is based on rate constants for the reactions of the OH-toluene adducts with O_2 and NO_2 of 5.7 x 10^{-16} cm^3 $molecule^{-1}$ s^{-1} and 3.6 x 10^{-11} cm^3 $molecule^{-1}$ s^{-1}, respectively (Knispel et al., 1990; Bohn, 2001).

IV. REFERENCES

Arey, J. 1998. Atmospheric reactions of PAHs including formation of nitroarenes. In *PAHs and Related Compounds*, A. H. Neilson, Ed. The Handbook of Environmental Chemistry, Volume 3, O. Hutzinger, Series Ed., Berlin: Springer-Verlag, pp. 347-385.

Arey, J. and R. Atkinson. 2003. Photochemical reactions of PAHs in the atmosphere: In *PAHs an Ecotoxicological Perspective*, P. E. T. Douben, Ed., West Sussex: John Wiley & Sons, Ltd., pp. 47-63.

Arey, J., B. Zielinska, R. Atkinson and A. M. Winer. 1987. Polycyclic aromatic hydrocarbon and nitroarene concentrations in ambient air during a wintertime high-NO_x episode in the Los Angeles basin. *Atmos. Environ.* 21: 1437-1444.

Arey, J., R. Atkinson, B. Zielinska and P. A. McElroy 1989. Diurnal concentrations of volatile polycyclic aromatic hydrocarbons and nitroarenes during a photochemical air pollution episode in Glendora, California. *Environ. Sci. Technol.* 23:321-327.

Arey, J., R. Atkinson, S. M. Aschmann and D. Schuetzle. 1990. Experimental investigation of the atmospheric chemistry of 2-methyl-1-nitronaphthalene and a comparison of predicted nitroarene concentrations with ambient air data. *Polycyclic Aromatic Compounds*. 1:33-50.

Arey, J., H. L. Bethel, F. Reisen and W. H. Brune. 2004. Nitro-PAHs in Mexico City: can their presence by attributed to hydroxyl radical reactions? Megacity Impacts on Air Quality, AGU Fall Meeting, San Francisco, CA, Dec. 13-5.

Atkinson, R. 1989. Kinetics and mechanisms of the gas-phase reactions of the hydroxyl radical with organic compounds. *J. Phys. Chem. Ref. Data.* Monograph 1:1-246.

Atkinson, R. 1991. Kinetics and mechanisms of the gas-phase reactions of the NO_3 radical with organic compounds. *J. Phys. Chem. Ref. Data.* 20:459-507.

Atkinson, R. 1994. Gas-Phase tropospheric chemistry of organic compounds. *J. Phys. Chem. Ref. Data*, Monograph 2: 1-216.

Atkinson, R. and S. M. Aschmann. 1994. Products of the gas-phase reactions of aromatic-hydrocarbons – effect of NO_2 concentration. *Int. J. Chem. Kinet.* 26: 929-944.

Atkinson, R. and J. Arey. 2003. Atmospheric degradation of volatile organic compounds. *Chem. Reviews*. 103:4605-4638.

Atkinson, R., S. M. Aschmann, W. P. L. Carter, A. M. Winer and J. N. Pitts, Jr., 1982. Alkyl nitrate formation from the NO_x-air photooxidations of C_2-C_8 *n*-alkanes. *J. Phys. Chem.*, 86, 4563-4569.

Atkinson, R., A. M. Winer and J. N. Pitts, Jr. 1986. Estimation of night-time N_2O_5 concentrations from ambient NO_2 and NO_3 radical concentrations and the role of N_2O_5 in night-time chemistry. *Atmos. Environ.* 20:331-339.

Atkinson, R., J. Arey, B. Zielinska and S. M. Aschmann. 1987. Kinetics and products of the gas-phase reactions of OH radicals and N_2O_5 with naphthalene and biphenyl. *Environ. Sci. Technol.* 21::1014-1022.

Atkinson, R., S. M. Aschmann, J. Arey and W. P. L. Carter. 1989. Formation of ring-retaining products from the OH radical-initiated reactions of benzene and toluene. *Int. J. Chem. Kinet.* 21:801-827.

Atkinson, R., S. M. Aschmann and J. Arey. 1991. Formation of ring-retaining products from the OH radical-initiated reactions of *o*-, *m*-, and *p*-xylene. *Int. J. Chem. Kinet.* 23:77-97.

Atkinson, R., E. C. Tuazon, I. Bridier and J. Arey. 1994. Reactions of NO_3-naphthalene adducts with O_2 and with NO_2. *Int. J. Chem. Kinet.* 26:605-614.

Atkinson, R., J. Arey, E. C. Tuazon, S. M. Aschmann, J. Sasaki and A. A. Chew. 1997. *Product Studies of the Atmospherically-Important Reactions of Selected VOCs*. Final Report to CRC-APRC Contract No. AQ-1-1-94, Coordinating Research Council.

Baker, J., J. Arey and R. Atkinson, 2004. Rate constants for the gas-phase reactions of OH radicals with a series of hydroxyaldehydes at 296 ± 2 K. *J. Phys. Chem. A* 108, 7032-7037.

Bethel, H. L., R. Atkinson and J. Arey. 2000. Products of the gas-phase reations of OH radicals with *p*-xylene and 1,2,3- and 1,2,4-trimethylbenzene: effect of NO_2 concentration. *J. Phys. Chem. A.* 104: 8922-8929.

Bidleman, T. F. 1988. Atmospheric processes. *Environ. Sci. Technol.* 22:361-367.

Bierbach, A., I. Barnes, K.H. Becker and E. Wiesen. 1994. Atmospheric chemistry of unsaturated carbonyls-butenedial, 4-oxo-2-pentenal, 3-hexene-2,5-dione, maleic-anhydride, 3H-furan-2-one, and 5-methyl-3H-furan-2-one. *Environ. Sci. Technol*. 28:715-729.

Bohn, B. 2001. Formation of peroxy radicals from OH-toluene adducts and O_2. *J. Phys. Chem. A.* 105:6092-6101.

Bohn. B. and C. Zetzsch. 1999. Gas-phase reaction of the OH-benzene adduct with O_2: reversibility and secondary formation of HO_2. *Phys. Chem. Chem. Phys.* 1:5097-5107.

Bunce, N. J., L. Liu, J. Zhu and D. A. Lane. 1997. Reaction of naphthalene and its derivatives with hydroxyl radicals in the gas phase. *Environ. Sci. Technol.* 31:2252-2259.

Calvert, J. G., R. Atkinson, K. H. Becker, R. M. Kamens, J. H. Seinfeld, T. J. Wallington and G. Yarwood. 2002. *The Mechanisms of Atmospheric Oxidation of Aromatic Hydrocarbons.* Oxford: Oxford University Press.

de Foy, B., E. Caetano, V. Magana, A. Zitacuaro, B. Cardenas, A. Retama, R. Ramos, L. T. Molina and M. J. Molina. 2005. Mexico City basin wind circulation during the MCMA-2003 field campaign. *Atmos. Chem. Phys.* 5:2267-2288.

Fraser, M. P., G. R. Cass and B. R. T. Simoneit. 1998. Gas-phase and particle-phase organic compounds emitted from motor vehicle traffic in Los Angeles roadway tunnel. *Environ. Sci. Technol.* 32:2051-2060.

Gupta, P., W. P. Harger and J. Arey. 1996. The contribution of nitro- and methylnitro-naphthalenes to the vapor-phase mutagenicity of ambient air samples. *Atmos. Environ.* 30:3157-3166.

Hoekman, S. K. 1992. Speciated measurements and calculated reactivities of vehicle exhaust emissions from conventional and reformulated gasolines. *Environ. Sci. Technol.* 26:1206-1216.

Klotz, B., I. Barnes and K. H. Becker. 1999. Kinetic study of the gas-phase photolysis and OH radical reaction of *E,Z* and *E,E*-2,4-hexadienedial. *Intern. J. Chem. Kinet*. 31:689-697.

Klotz, B., R. Volkamer, M. D. Hurley, M. P. S. Andersen, O. J. Nielsen, I. Barnes, T. Imamura, K.Wirtz, K.-H. Becker, U. Platt, T. J. Wallington and N. Washida. 2002. OH-initiated oxidation of benzene. Part II. Influence of elevated NO_x concentrations. *Phys. Chem. Chem. Phys.* 4:4399-4411.

Klotz, B. G., A. Bierbach, I. Barnes and K. H. Becker. 1995. Kinetic and mechanistic study of the atmospheric chemistry of muconaldehydes. *Environ. Sci. Technol*. 29:2322-2332.

Knispel, R., R. Koch, M. Siese and C. Zetzsch. 1990. Adduct formation of OH radicals with benzene, toluene, and phenol and consecutive reactions of the adducts with NO_x and O_2. *Ber. Bunsenges. Phys. Chem.* 94:1375-1379.

Koch, R., R. Knispel, M. Siese and C. Zetzsch. 1994. Absolute rate constants and products of secondary steps in the atmospheric degradation of aromatics: In *Proceedings of the 6th European Symposium on the Physico-Chemical Behavior of Atmospheric Pollutants,* G. Angeletti and G. Restelli, Eds., European Commission, pp. 143-149.

Krol, M. and J. Lelieveld. 2003. Can the variability in tropospheric OH be deduced from measurements of 1,1,1-trichloroethane (methyl chloroform)? *J. Geophys. Res.* 108: doi:10.1029/2002JD002423.

Kwok, E. S. C. and R. Atkinson, 1995. Estimation of hydroxyl radical reaction-rate constants for gas-phase organic-compounds using a structure-reactivity relationship – an update. *Atmos. Environ*. 29: 1685-1695.

Kwok, E. S. C.; S. M. Aschmann, R. Atkinson, and J. Arey. 1997. Products of the gas-phase reactions of *o*-, *m*-, and *p*-xylene with the OH radical in the presence and absence of NO_x. *J. Chem. Soc. Faraday Trans.*, 93:2847-2854.

Magneron, I., R. Thévenet, A. Melloiki, G. Le Bras, G. K. Moortgat and K. Wirtz. 2002. A study of the photolysis and OH-initiated oxidation of acrolein and trans-crotonaldehyde. *J. Phys. Chem. A* 106: 2526-2537.

Marr, L. C., T. W. Kirchstetter, R. A. Harley, A. H. Miguel, S. V. Hering and S. K. Hammond. 1999. Characterization of polycyclic aromatic hydrocarbons in motor vehicle fuels and exhaust emissions. *Environ. Sci. Technol.* 33:3091-3099.

Marr, L. C., K. Dzepina, J. L. Jimenez, F. Reisen, H. L. Bethel, J. Arey, J. S. Gaffney, N. A. Marley, L. T. Molina and M. J. Molina. 2006. Sources and transformations of particle-bound polycyclic aromatic hydrocarbons in Mexico City. *Atmos. Chem. Phys.* 6:1733-1745.

Martos, P.A. and J. Pawliszyn. 1998. Sampling and determination of formaldehyde using solid-phase microextraction with on-fiber derivatization. *Anal. Chem.* 70: 2311-2320.

Odum, J. R., T. P. W. Jungkamp, R. J. Griffin, R. C. Flagan and J. H. Seinfeld. 1997. The atmospheric aerosol-forming potential of whole gasoline vapor. *Science* 276: 96-99.

OEHHA. 2006. *Atmospheric Chemistry of Gasoline-Related Emissions: Formation of Pollutants of Potential Concern.* Reproductive and Cancer Hazard Assessment Branch, Office of Environmental Health Hazard Assessment, California Environmental Protection Agency, January.

Orlando, J. J. and G. S. Tyndall. 2002. Mechanisms for the reactions of OH with two unsaturated aldehydes: crotonaldehyde and acrolein. *J. Phys. Chem. A* 106: 12252-12259.

Orlando, J. J., G. S. Tyndall and S. E. Paulson. 1999. Mechanism of the OH-initiated oxidation of methacrolein. *Geophys. Res. Lett.* 26:2191-2194.

Orlando, J. J., G. S. Tyndall, S. B. Bertman, W. Chen and J. B. Burkholder. 2002. Rate coefficient for the reaction of OH with $CH_2=C(CH_3)C(O)OONO_2$ (MPAN). *Atmos. Environ*. 36:1895-1900.

Phousongphouang, P. T. and J. Arey. 2002. Rate constants for the gas-phase reactions of a series of alkylnaphthalenes with the OH radical. *Environ. Sci. Technol.* 36:1947-1952.

Phousongphouang, P. T. and J. Arey. 2003a. Rate constants for the gas-phase reactions of a series of alkylnaphthalenes with the nitrate radical. *Environ. Sci. Technol.* 37:308-313.

Phousongphouang, P. T. and J. Arey. 2003b. Rate constants for the photolysis of the nitronaphthalenes and methylnitronaphthalenes. *J. Photochem. Photobiol. A: Chemistry.* 157:301-309.

Prinn, R. G., J. Huang, R. F. Weiss, D. M. Cunnold, P. J. Fraser, P. G. Simmonds, A. McCulloch, C. Harth, P. Salameh, S. O'Doherty, R. H. J. Wang, L. Porter and B. R. Miller. 2001. Evidence for substantial variations of atmospheric hydroxyl radicals in the past two decades. *Science*. 292:1882-1888.

Reisen, F. 2003. Atmospheric Chemistry and Measurements of Vehicle-derived Polycyclic Aromatic Compounds. Ph.D. Thesis, University of California, Riverside.

Reisen, F. and J. Arey. 2005. Atmospheric reactions influence seasonal PAH and Nitro-PAH concentrations in the Los Angeles basin. *Environ. Sci. Technol.* 39:64-73.

Reisen, F., S. Wheeler and J. Arey. 2003a. Methyl and dimethyl-/ethyl- nitronaphthalenes measured in ambient air in Southern California. *Atmos. Environ.* 37:3653-3657.

Reisen , F., S. M. Aschmann, R. Atkinson and J. Arey, 2003b. Hydroxyaldehyde products from the hydroxyl radical reactions of *Z*-3-hexene-1-ol and 2-methyl-3-buten-2-ol quantified by SPME and API-MS. *Environ. Sci. Technol*., 37, 4664-4671.

Reisen, F., S. M. Aschmann, R. Atkinson and J. Arey, 2005. 1,4-Hydroxycarbonyl products of the OH radical-initiated reactions of C_5-C_8 *n*-alkanes in the presence of NO_x. *Environ. Sci. Technol.* 39:4447-4453.

Sasaki, J., S. M. Aschmann, E. S. C. Kwok, R. Atkinson and J. Arey. 1997. Products of the gas-phase OH and NO_3 radical-initiated reactions of naphthalene. *Environ. Sci. Technol.* 37:173-3179.

Smith, D. F., T. E. Kleindienst and C.D. McIver. 1999. Primary product distributions from the reaction of OH with m-, p-xylene, 1,2,4- and 1,3,5-trimethylbenzene. *J. Atmos. Chem*. 34:339-364.

Tancell, P. J., M. M. Rhead, R. D. Pemberton and J. Braven. 1995. Survival of polycyclic aromatic hydrocarbons during diesel combustion. *Environ. Sci. Technol.* 29:2871-2876.

Taylor, W. D., T. D. Allston, M. J. Moscato, G. B. Fazekas, R. Kozlowski and G. A. Takacs, 1980. Atmospheric photodissociation lifetimes for nitromethane, methyl nitrite, and methyl nitrate. *Int. J. Chem. Kinet*., 12: 231-240.

Tuazon, E. C. and R. Atkinson, 1989. A product study of the gas-phase reactions of methyl vinyl ketone with the OH radical in the presence of NO_x. *Int. J. Chem. Kinet*., 21: 1141-1152.

Tuazon, E. C. and R. Atkinson, 1990. A product study of the gas-phase reactions of methacrolein with the OH radical in the presence of NO_x. *Int. J. Chem. Kinet*., 22: 591-602.

Volkamer, R., U. Platt and K. Wirtz. 2001. Primary and secondary glyoxal formation from aromatics: experimental evidence for the bicycloalkyl-radical pathway for benzene, toluene and *p*-xylene. *J. Phys. Chem. A.* 105:7865-7874.

Volkamer, R., P. Spietz, J. Burrows and U. Platt. 2005. High-resolution absorption cross-section of glyoxal in the UV-vis and IR spectral ranges. *J. Photochem. Photobiol. A: Chemistry*. 172:35-46.

Wania, F. and D. Mackay. 1996. Tracking the distribution of persistent organic pollutants. *Environ. Sci. Technol.* 30:A390-A396.

Williams, P. T., M. K. Abbass and G. E. Andrews. 1989. Diesel particulate emissions: the role of unburned fuel. *Combustion and Flame*. 75:1-24.

Winer, A. M., R. Atkinson, J. Arey, H. W. Biermann, W. P. Harger, E. C. Tuazon, B. Zielinska. 1987. *The Role of Nitrogenous Pollutants in the Formation of Atmospheric Mutagens and Acid Deposition.* Final Report to the California Air Resources Board, Contract No. A4-081-32, March.

Yu, J., H.E. Jeffries and K.G. Sexton. 1997. Atmospheric photooxidation of alkylbenzenes .1. carbonyl product analyses. *Atmos. Environ.* 31:2261-2280.

Yu, J. and H.E. Jeffries. 1997. Atmospheric photooxidation of alkylbenzenes .2. evidence of formation of epoxide intermediates. *Atmos. Environ.* 31:2281-2287.

Zielinska, B., J. Arey, R. Atkinson and P. A. McElroy. 1989. Formation of methylnitronaphthalenes from the gas-phase reactions of 1- and 2-methylnaphthalene with OH radicals and N_2O_5 and their occurrence in ambient air. *Environ. Sci. Technol.* 23:723-729.

Zielinska, B., J. Sagebiel, J. D. McDonald, K. Whitney and D. R. Lawson. 2004. Emission rates and comparative chemical composition from selected in-use diesel and gasoline-fueled vehicles. *J. Air & Waste Manage. Assoc.* 54:1138-1150.

V. GLOSSARY

CH_3ONO	Methyl nitrite
CO	Carbon monoxide
CO_2	Carbon dioxide
F	Multiplicative factor to take into account secondary reactions
FT-IR	Fourier transform infrared
GC-FID	Gas chromatography with flame ionization detection
GC-MS	Combined gas chromatography-mass spectrometry
GC-NICIMS	Combined gas chromatography-negative ion chemical ionization mass spectrometry
HO_2	Hydroperoxyl radical
IR	Infrared
k_a	Rate constant for reaction pathway A
MN	Methylnaphthalene
MNN	Methylnitronaphthalene
NCI	Negative chemical ionization
nm	Nanometer (10^{-9} m)
NO	Nitric oxide
NO_2	Nitrogen dioxide
NO_3	Nitrate radical
OH	Hydroxyl radical
O_3	Ozone
PAH	Polycyclic aromatic hydrocarbon

PFBHA	*O*-(2,3,4,5,6-Pentafluorobenzyl)hydroxylamine
$R^{\bullet}$	Alkyl or substituted alkyl radical
$RC(O)OO^{\bullet}$	Peroxyacyl radical
$RC(O)OONO_2$	Peroxyacyl nitrate
$RO^{\bullet}$	Alkoxy radical
$ROO^{\bullet}$ or $RO_2^{\bullet}$	Alkyl peroxy radical
SIM	Single ion monitoring
SPME	Solid phase micro extraction
VOC	Volatile organic compound